High energy cosmic ray neutrons

Smith, N. I.

PLATE 1

FRONTISPIECE

FRONT VIEW OF APPARATUS

USED TO MEASURE THE NEUTRON SPECTRUM

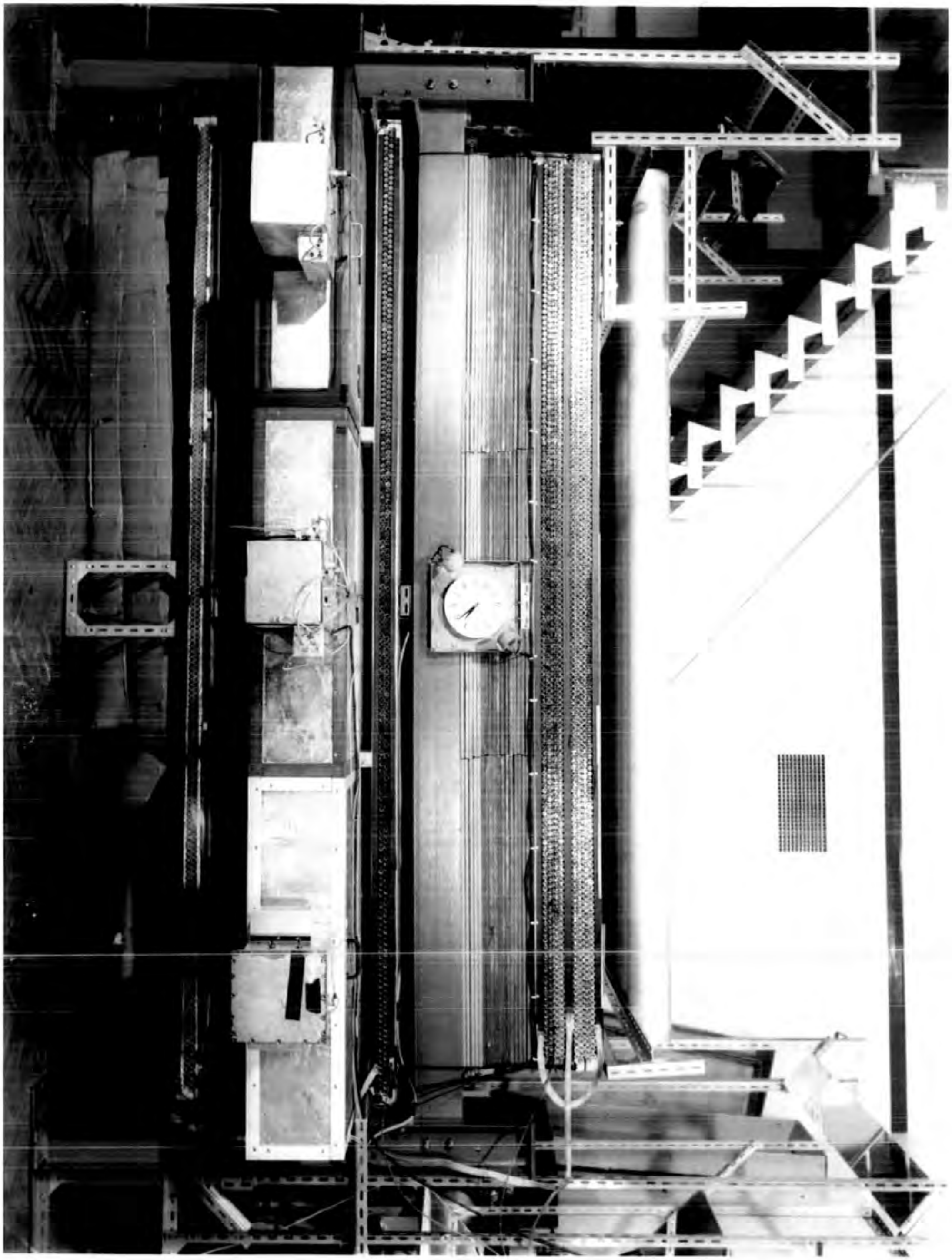

HIGH ENERGY COSMIC RAY NEUTRONS

by

N.I. Smith, B.Sc.

A Thesis submitted to the

University of Durham

for the Degree of Doctor of Philosophy

December, 1969.

CONTENTS

ABSTRACT

A measurement of the sea level energy spectrum of cosmic ray neutrons in the energy range 50-1000 GeV has been performed. The neutrons interacted in a thick iron absorber, the burst subsequently produced being detected by a scintillation counter. The burst sizes were used to select events and to estimate the energy of the neutrons. The experimental results show a neutron spectrum that is steeper ($\gamma = 2.95 \pm 0.1$) than might normally be expected. This has been discussed in terms of nucleon propagation in the atmosphere. One possible explanation would be a decrease in the nucleon attenuation length in the atmosphere. An alternative solution is in terms of the charge exchange probability for nucleon interactions. If, as has recently been postulated, the Aleph baryon is produced in high energy (> 1000 GeV) nucleon collisions, this would lead to a deficit in the expected number of neutrons at sea level in the energy range covered by this experiment.

A search for high energy magnetic monopoles has been made using the same apparatus. No events satisfying the selection requirements were observed and the upper limit to the flux at the 90% confidence level is $< 9.5. \ 10^{-11}$ cm^{-2} sec^{-1} sterad^{-1}.

An investigation of the characteristics of long cylindrical proportional and sonic spark counters has also been carried out.

PREFACE

This thesis describes the work performed by the author in the Physics Department of the University of Durham while he was a Research Student under the supervision of Dr. F. Ashton.

An experiment to measure the sea level energy spectrum of cosmic ray neutrons has been performed. The construction, day-to-day running of the apparatus, analysis and interpretation of the data have been the sole responsibility of the author with the assistance in some of the early work from Mr. J. King.

Results of the experiment have been presented at the International Conference on Cosmic Rays at Budapest by Ashton et al (1969).

The author, along with Mr. T. Takahashi, has investigated the properties of long cylindrical proportional counters and sonic spark counters. A paper giving details of the characteristics of these counters has been reported by Ashton et al (1967) at the Calgary Conference on Cosmic Rays.

CHAPTER 1

INTRODUCTION

1.1. General

Over the past century or so it has become increasingly obvious that the basic units from which matter is thought to be composed have grown smaller and smaller, and the various forces involved more complex. Around 1930 it was believed that all the then known physical phenomena could be explained on the basis of just three elementary particles - the proton, the electron and the photon - interacting through two basic types of force - electromagnetic and gravitational. The electrons and protons were treated as structureless points, defined by their mass and charge with both of the fundamental interactions - the gravitational attraction between masses and the Coulomb force between charges - being long range interactions, falling off inversely as the square of the distance. The strength of the Coulomb interaction between two protons is characterised by the pure number $e^2/\hbar c$ which is known as the fine structure constant its value being 1/137. The corresponding number for the strength of the gravitational force between protons is 10^{-36} so it can be seen that this force plays no significant part in nuclear phenomena.

It soon became clear that phenomena in the nucleus lay outside this scheme. The typical nuclear radius is about 10^{-12}cm. and

consequently the Coulomb repulsion between a pair of protons is the nucleus is about 10^8 times as large as the attraction between the nucleus and the atomic electrons. The gravitational force has been shown to be negligible on this scale so it became necessary to postulate a new type of force - the nuclear force - in order to explain the observed stability of nuclei. This force has a strength of about 1 on the above scale. In 1932 the neutron had been discovered and in order to account for the mass to charge ratio of nuclei it was assumed they were composed of approximately equal numbers of protons and neutrons. It seemed reasonable to assume that both types of particle, collectively known as nucleons, were subject to this nuclear force. Observations on the nucleon number and nuclear binding energy indicated that the nuclear force operated only between nearest neighbours giving it a range of only about 10^{-13}cm. Within this radius it operates very strongly but falls off very rapidly at larger distances.

In the past thirty years the nuclear force has been the subject of intensive study. Unlike the electromagnetic interaction, the knowledge of which has become relatively complete, the nuclear interaction is still without a satisfactory description. The chief method of investigation has been the study of collisions between nucleons with the aid of accelerators and detectors such as bubble chambers. The resulting nuclear model has developed from an original idea of Yukawa (1935). By analogy with the photon which was the

exchange particle involved in the electromagnetic interaction he postulated the pi-meson as intermediary in a nuclear reaction. This particle was subsequently discovered in cosmic rays and it became clear that the protons and neutrons were not structureless points but clusters of sub-nuclear material of radius about 10^{-13}cm. Essentially no interaction occurred unless these clusters came into contact when a very strong interaction took place. This interaction occurs in a very short time - about 10^{-23} seconds - and is best described by the exchange of material from one nucleon to the other. The lightest of these fragments is the pi-meson. Since the discovery of this particle a wide spectrum of sub-nuclear particles has been revealed and the understanding and classification of these has become one of the major problems of fundamental physics. Considerable advances have been made in this field by studying the various conservation laws that apply in the particle interactions. There are three such laws that apply to strong interactions. The first, the conservation of electric charge C, is thought to be an absolute conservation law. The second law is that of baryonic charge B. This was first suggested by the abundance of protons in the universe and was formulated to account for their stability. This law is again thought to be absolute and universally applicable. A third rule that applies only to the strong interation is the conservation of a quantity known as the hypercharge Y. This arose from the observation that when Λ or Σ baryons were produced in pion-nucleon collisions

they were always accompanied by an equal number of positive K mesons.

The problem then arises as to what mechanism could most simply give rise to these observed regularities. One such scheme is the proposal that the nuclear particles can themselves be thought of as being made up of sub-nuclear particles, called quarks, which carry the differant charges C,B,Y. The suggestion is that there are three such quarks (charges +2/3, -1/3, -1/3) each with spin 1/2. The half integral spin particles are then a tightly bound combination of three quarks, and zero and integral spin particles a tightly bound system of a quark and an anitquark. Under the theory of unitary symmetry which accounts for the charges on the particles but not for the conservation laws the quark content of any system has to be conserved. Under this theory it seems that the great multiplicity of nuclear particles has been brought into some sort of order, the unitary multiplets being closely analogous to the periods of the chemical elements in the Periodic Table.

The question can then be posed as to whether quarks actually exist as sub-nuclear elements or whether they are merely a convenient mathematical invention. Various experiments at accelerators and in cosmic rays have been performed but although the search has been extremely extensive no quarks have been found. Thus the physical existence of quarks remains in doubt and the search is still for a simple basis to a complete understanding of the sub-nuclear world.

1.2 Study of Nuclear Interactions in Cosmic Rays

The important role of energy in revealing new phenomena in the interaction of elementary particles gives cosmic ray physicists the advantage, in comparison with accelerator physicists, of being pioneers in this field of research because cosmic ray particles are always available up to practically infinite energy. In the past twenty years many fundamental phenomena have been observed and measured in cosmic rays. For example the existence of π and μ mesons and of several strange particles, the average multiplicities and the constancy of the average transverse momentum of secondaries have all been established. It should be pointed out, however, that as proton accelerators have increased in energy up to around 30 GeV they have yielded much more accurate knowledge than could ever hoped to be gained from cosmic ray studies. In brief it would appear that cosmic ray research can lead to the discovery of phenomena which are of fundamental importance for the understanding of high energy interactions but whenever accelerators can cover the same energy range the cosmic ray evidence is qualitatively and quantitatively inferior.

As the accelerators reach higher energy the problem of studying high energy interactions in cosmic rays becomes progessively more difficulty since the flux levels are so small. Obviously the largest flux of protons is to be found in the primary radiation and in recent years the use of satellites has enabled measurements here to

be made over long periods of time. For example the "Proton" series of flights have enabled the primary spectrum to be determined directly up to energies in excess of 10^{14}eV / nucleon and measurements of the elementary p-p inelastic cross-section have been made up to above 100 GeV.

Experiments to study the various cosmic ray spectra at different depths in the atmosphere enable the propagation of nucleons through the atmosphere to be studied. It is possible, for example, to make an estimate of the attenuation length of nucleons if the primary nucleon spectrum is known. This can lead to a value for the elasticity of nucleon-air nucleus collisions assuming a reliable estimate of the nucleon interaction length in air is available. In the present work the spectrum of neutrons at sea-level has been measured in an effort to detect any energy dependence of these parameters.

1.3. Measurement of the High Energy Neutron Spectrum

Previous measurements of sea level nucleon spectra above 1 GeV appear to have been confined almost entirely to protons. The best measurement here is that of Brooke et al (1964) who used a magnetic spectrograph to estimate the proton spectrum up to about 80 GeV. No comparable studies of the neutron spectrum have been made.

This thesis describes an experiment to measure the high energy neutron spectrum from a study of the cascades produced by neutron interactions in an iron target. A particular advantage of the experiment

lies in the fact that the neutrons are easily identified as there is no background from other neutral particles. In the case of protons they have to be separated out from the pion and muon components.

The apparatus which is described in detail in Chapter 6 consisted of an iron target in which incoming particles interacted. Situated below the iron were three large scintillation counters whose pulse height information enabled the energy of the interacting particles to be estimated. Visual information about the cascade was obtained from crossed trays of flash tubes above and below the scintillator and the nature of the incoming particle (charged or uncharged) was determined from a tray of flash tubes above the iron target.

In Chapter 2 a review of the primary spectrum measurements is given together with an estimate of the primary nucleon spectrum. The propagation of nucleons through the atmosphere is discussed in Chapter 3 and measurements of the nuclear active particle spectrum at various atmospheric depths in Chapter 4. The theory of burst production in iron is given in Chapter 5 while in Chapter 6 the details of the apparatus and experimental data are described. The measured sea level neutron spectrum is discussed in Chapter 7 and concluding remarks made in Chapter 8.

Appendix A discusses the monopole flux at sea level while in Appendix B the development of large proportional counters and sonic spark counters is described.

CHAPTER 2

REVIEW OF PRIMARY SPECTRUM MEASUREMENTS

2.1 Introduction

A knowledge of the primary spectrum of cosmic rays is important for the following two reasons:

a) in the interpretation of the phenomena of high energy physics e.g. muon production, cross-sections and elasticities of high energy nuclear interactions.

b) in the study of the astrophysical and geophysical aspects of cosmic rays, e.g. their origin, acceleration and time variations.

The techniques used in the measurement of the spectrum and the accuracy of its determination vary considerably according to the energy range involved. At energies of about 20 GeV and less where the influence of the earth's magnetic field is noticeable the spectrum can be measured directly using geomagnetic techniques. These are usually performed with balloons or, as in more recent years, satellites carrying emulsions or counters. It is at this low energy region that solar influences on the spectrum are most marked. This is seen in the neutron monitor counting rates which are in anticorrelation with the 11-year cycle of sunspot activity. In the energy range 10^{11} to 10^{14}eV / nucleon measurements have been confined almost exclusively to studying interactions occurring in nuclear emulsions, although recently Grigorov

et al (1967) have used satellites containing ionisation calorimeters. Above 10^{14} eV / nucleon the primary spectrum has to be derived from measurements on the size of extensive air showers. This last indirect method enables the spectrum to be estimated up to an energy of about 10^{20} eV / nucleon although at these energies the errors are quite large as few events have been observed.

2.2 The Total Radiation Spectrum

2.2.1 Latitude Sensitive Region

The most direct measurements on the total radiation spectrum are those in the latitude sensitive region. These involve the use of counters or ionisation chambers at or near the top of the atmosphere and are dependent on a knowledge of the correct geomagnetic cut-off as a function of latitude. Measurements at the low energy end of the spectrum have been performed using the latitude effect by Neher (1961) using ion chambers and by Lin et al (1963) using a single counter. The counter measurements were made in a satellite at an altitude of about 1000 km. and the data was adjusted to the top of the atmosphere by taking into account the fraction of the intensity due to albedos. The accuracy of the absolute intensities in this energy region depends mainly on the albedo correction and this is the chief source of disagreement between the various measurements. Albedo intensities have been studied by McDonald and Webber (1959) - the splash albedo - and by Perlow et al (1952) - the re-entrant albedo. Using these corrections, Webber (1967)

estimates the integral total radiation spectrum in this energy region (3.5 - 20 GeV / nucleon) at sunspot minimum and this is shown in Fig. 2.1.

2.2.2 Indirect Methods

In the energy range 100-1000 GeV / nucleon the total radiation spectrum has been derived from the measured spectrum of γ-rays at high altitudes. Measurements on electromagnetic cascades produced high in the atmosphere have been performed by Duthie et al (1962) and Kidd (1963) both using balloons. Since these cascades are thought to originate from secondary γ-rays, an estimate of the pion production spectrum is then possible. Assuming a model for the primary nucleon - air nucleus collision the integral spectrum of primary particles can then be derived. This method has been used by Miyake (1963) who found a spectrum of exponent -1.63 constant in the energy interval 500-1000 GeV / nucleon (Fig. 2.1). Malholtra et al (1965) have flown emulsion stacks in a balloon at an atmospheric depth of 22gm. cm^{-2}. The integral spectrum of cascades initiated by nuclear active particles was measured and this was used to derive the primary spectrum. They estimate that between 10^{11} and 6.10^{14}eV/ nucleon the primary spectrum of all nuclei can be represented by

$$N(>E) = (3.9^{+3.4}_{-1.8}).\ 10^{14}\ E^{-1.60\pm0.01}\ cm.^{-2}\ sec.^{-1}\ sterad.^{-1}$$

where E is in eV. This is shown in Fig. 2.1.

Brooke et al (1964b) have also used an indirect method based on

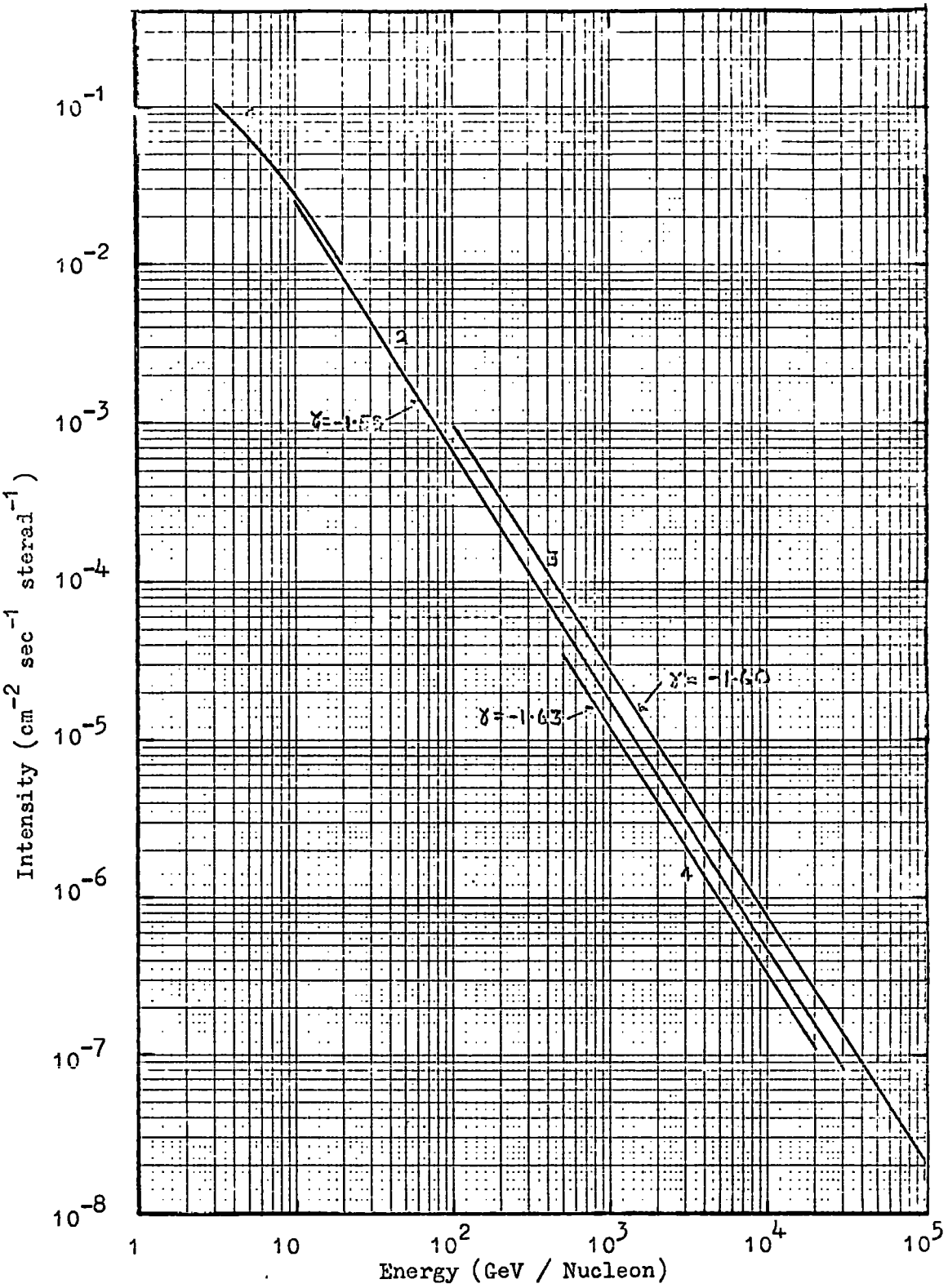

Figure 2.1 Total Radiation Spectrum.

1. Webber (1967).
2. Brooke et al. (1964b).
3. Malholtra et al. (1965).
4. Miyake (1963).

the measured sea level spectra of cosmic ray protons and muons. Using these spectra, it is possible to draw quantitative conclusions about the primary spectrum if a model is assumed for the interaction between a primary nucleon and an air nucleus. In this case the C.K.P, model for high energy nucleon-interactions was adopted and a constant value of the quantity $(K_t - K_\pi)$ was assumed where K_t was the nucleon inelasticity and K_π the fraction of energy passed on to pions. Taking into account geomagnetic measurements the integral spectrum in the range 10^{10} -3.10^{13} eV / nucleon was found to be given by the expression

$$N(>E) = (0.87^{+0.52}_{-0.30})\ E^{-1.58}\ cm^{-2}\ sec^{-1}\ sterad^{-1}$$

with E in GeV. The spectrum is shown in Fig 2.1.

It can be seen from Fig. 2.1. that these indirect methods give agreement on the exponent of the spectrum although there is a discrepancy in the absolute intensities. The errors, however, are quite large and the spectra lie within each others uncertainties.

2.3 The Primary Proton Spectrum

2.3.1 Direct Measurements

The singly charged particles (protons) are the most abundant present in the primary spectrum. It is, however, only in the region up to about 10 GeV / nucleon that the energy of this component has been uniquely determined. Above this energy the spectrum is measured as an integral intensity above some rigidity determined by the geomagnetic

cut-off of the particular location. At energies above the latitude sensitive region the integral spectrum is studied from interactions in emulsions.

In the energy region below 1 GeV / nucleon Webber (1967) gives a summary of the measurements made up to 1963. Most of these point to a differential proton primary spectrum that is rising with increasing energy in the range 150-350 MeV / nucleon and reaches a peak at around 450 MeV / nucleon. There is some discrepancy, however, in the values of the absolute rates. This is thought to be due to the fact that most of the measurements have been carried out at a depth of a few gm.cm.$^{-2}$ into the earth's atmosphere. This makes it difficult to identify the separate components as there is a large background of secondaries produced in the overlying atmosphere as well as the contributions of the splash and re-entrant albedos. Of five measurements made in 1963, four are in quite good agreement and they give a differential spectrum which exhibits the features mentioned above. Above 450 MeV the spectrum starts to fall with increasing energy.

More recently Gloeckler and Jokipii (1967) have collected together various balloon and satellite data which refer to a time near a solar minimum of 1965 (Fig. 2.2.). The combined data shows a peak in the spectrum at an energy of just greater than 400 MeV / nucleon with a falling-off in intensity towards lower energies. They also indicate, however, that the spectrum reaches a minimum at about 30 MeV / nucleon and there is some evidence that it increases with decreasing energy

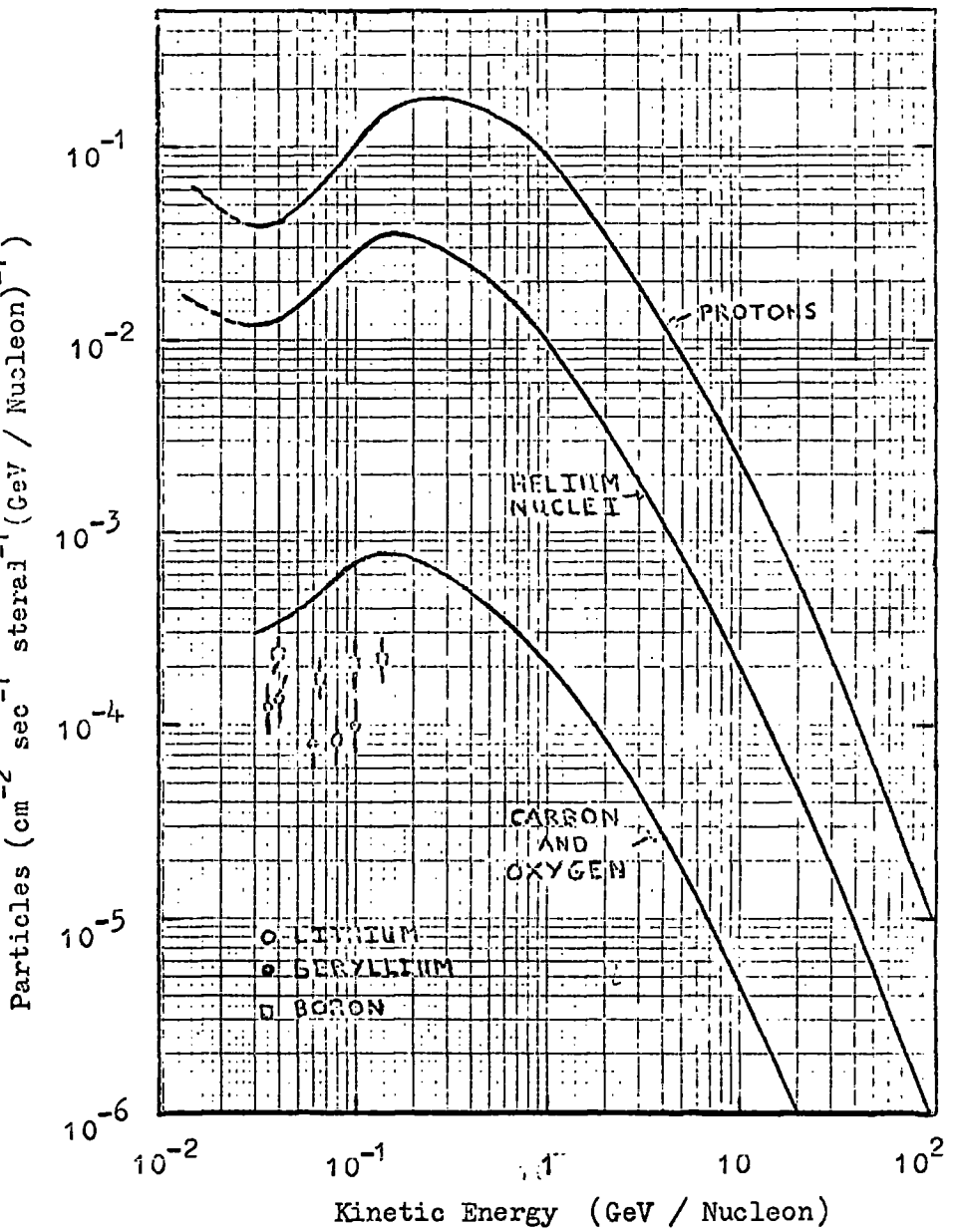

Figure 2.2 Differential Primary Spectrum of various Nuclei.

Protons and Helium Nuclei - Gloeckler and Jokipii (1967).

Carbon, Oxygen, etc. - Fan et al. (1967).

below this.

In the latitude sensitive region above about 500 MeV / nucleon the data of Webber and of Gloeckler and Jokipii show a falling spectrum whose exponent increases with increasing energy up to energies in excess of 10 GeV / nucleon.

In these regions of quite low energies it is not realistic to compare the absolute intensities of the two sets of data as they refer to slightly differing times and so may be affected differently by modulation. There is, however, quite good agreement between the two especially with regard to the general shape of the spectram.

2.3.2 Measurements in the range 10^{11} - 10^{14} eV / nucleon

The integral primary proton spectrum has been measured in this energy range almost exclusively from the study of interactions in emulsions. This method can lead to an uncertainty in the energy determination amounting to about a factor of two or three. The points of Lal (1953), Kaplon et al (1952), Appa Rao et al (1963) and Teucher (1960) as shown in Fig. 2.3. all lie on a straight line whose exponent is -1.6, but the absolute intensities are a factor of three higher than the total radiation spectrum discussed in section 2.2. This discrepancy could be due to an overestimate of the primary energy and while it should be remembered that the total radiation spectra at these energies were obtained in an indirect manner, they do agree quite well with the direct measurements of the proton spectra at lower energies.

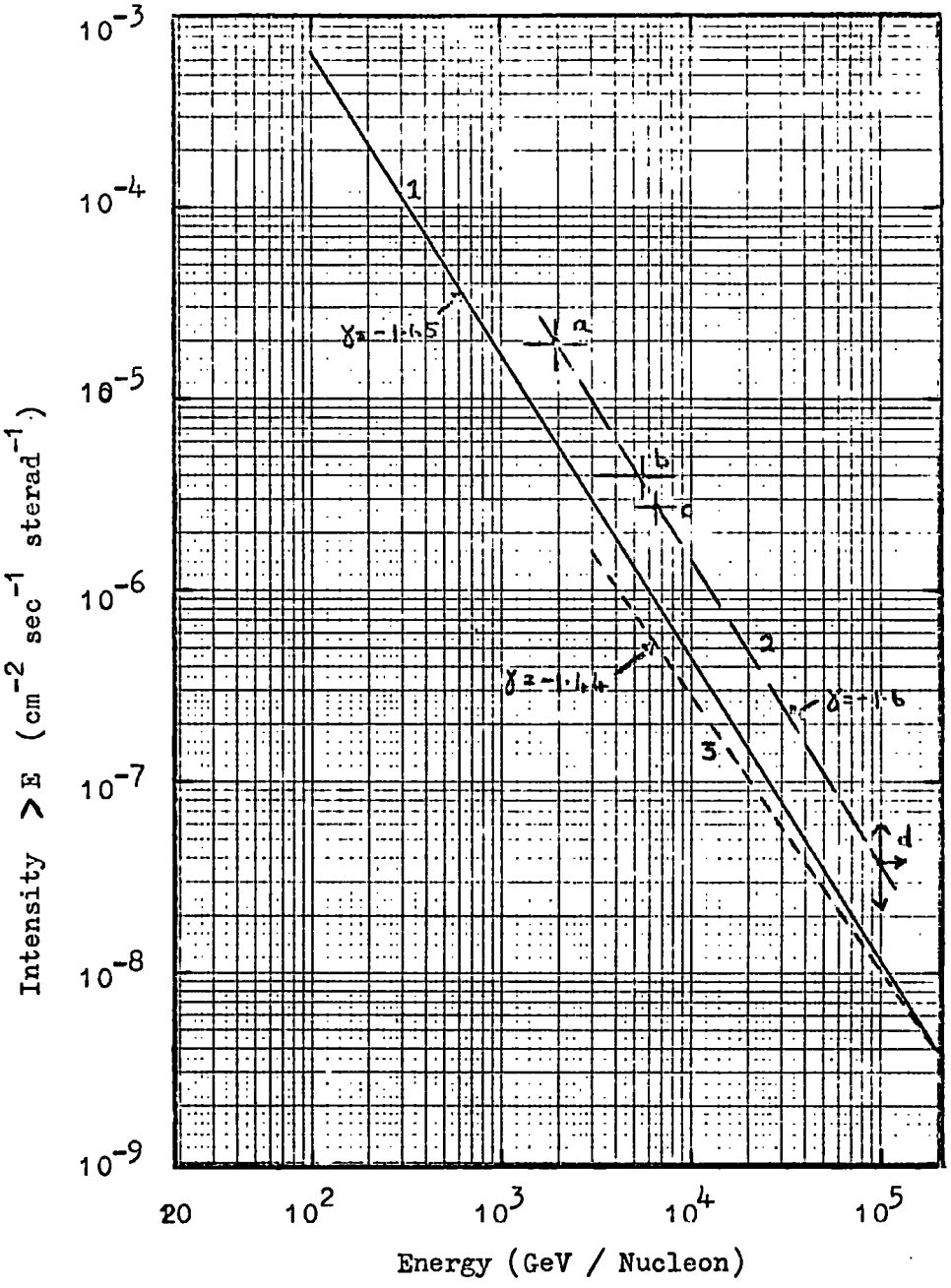

Figure 2.3 Integral Spectrum of Primary Protons in the energy range 10^2 to 10^5 GeV.

a: Lal (1953). b: Kaplon et al. (1952).
c: Appa Rao et al. (1963). d: Teucher (1960).
1: Extrapolation of Proton Spectrum given by Gloeckler and Jokipii (1967).
2: Best fit to emulsion data.
3: Malholtra et al. (1965).

Malholtra et al (1965) have used their measured spectrum of nuclear active particles to estimate the primary proton spectrum. They estimated the charge composition of the primaries in two ways: (a) Most of the interactions took place in tungsten but a few did occur in the emulsion itself and the composition was estimated from these. (b) It was assumed that at high energies the charge composition at the top of the atmosphere is the same as at low energies. The two estimates were found to be in good agreement and they thus conclude there is no evidence for a change in composition between 10^{10} and 10^{13} eV / nucleon. They obtain the following expression for integral spectrum of primary protons, in the range $2.6.\ 10^{12}$ to $2.6.\ 10^{14}$ eV / nucleon.

$$N(>E) = (1.67 \pm 0.06) 10^{12}\ Ep^{-1.44 \pm 0.05}$$

where Ep is in eV. This is shown in Fig 2.3.

Gloeckler and Jokipii have extended their differential spectrum of primary protons up to 100 GeV from measured integral flux values. (Fig. 2.2.). It is interesting to note that at 100 GeV their spectrum agrees both in absolute intensity and exponent with the total radiation spectrum calculated by Brooke et al.

2.3.3 Primary Proton Spectrum at $> 10^{14}$ eV / nucleon

Above about 10^{14} eV / nucleon it is not really possible to measure the primary proton spectrum as the intensities become much too small. In this energy region the primary spectrum is derived from

extensive air shower measurements and refers to a spectrum of all particles although it is possible to make inferences regarding the composition. It is worthwhile pointing out here in connection with the intensity of protons measured in emulsion stacks that the intensities from air shower data seem to be more compatible with the derived total radiation spectrum.

2.4 The Spectrum of Helium Nuclei.

2.4.1 Energies $\leq$10 GeV / nucleon

The spectrum of helium nuclei has been studied in detail by several groups in the low energy region. The helium nuclei are easily identified in the emulsions and counters since there is no contribution from albedos. The spectrum is thus quite well defined and in fact is known more precisely than that of the proton component even though the intensities are less. As with protons less experimental data is available at higher energies and there are no direct measurements above 10^{13} eV / nucleon.

At the very low energy end of the spectrum Webber (1967) groups the experimental results from two different periods, 1954-56 and 1963, when the solar modulation effects were reasonably small. The results for the 1954-56 period were taken from three emulsion and four counter experiments and the two sets of data (emulsion and counter) were found to be consistent over the energy range involved, 200 -800 MeV / nucleon. The measurements show a spectrum that is

falling with a constant exponent above about 400 MeV / nucleon but which below this energy has an ever decreasing slope and eventually appears to flatten out at around 200 MeV / nucleon.

The information available from the 1963 group of measurements is much more extensive and also covers a wider energy range. Again emulsion and counter type experiments were performed and the shape of the spectrum was found to be very similar to that of protons in the same energy range. Up to about 150 MeV / nucleon the spectrum rises with increasing energy, reaches a maximum at around 150 MeV / nucleon and then starts to fall as the energy goes up further. The absolute intensities from the 1963 series of experiments are in agreement with the 1954-56 measurements.

Gloeckler and Jokipii (1967), Fig. 2.2, also give quite extensive data on the helium spectrum in this energy region and the shape is in good agreement with the results previously discussed. It shows a maximum at around 150 MeV / nucleon below which the spectrum falls with decreasing energy. As in the case of the proton spectrum there is evidence for a minimum at about 40 MeV / nucleon.

In the energy region 1.5 - 10 GeV / nucleon there are balloon measurements by Ormes and Webber (1966) and by Arnand et al (1966). Both of these were carried out at a time near a solar minimum and they point to a falling spectrum whose slope is increasing slightly with increasing energy up to about 10 GeV / nucleon.

2.4.2 Energies > 10 GeV / nucleon

Over the range 10^{11} - 10^{13} eV / nucleon the only direct method of studying the primary spectrum of helium nuclei has been to look at their interactions in emulsions. This can lead to inaccuracies in the energy determination as was seen in the case of proton measurements. There are measurements by Fowler et al (1956), Lohrmann et al (1959) and by Jain et al (1959) and these points are plotted in Fig. 2.4. It can be seen that the three points do not lie on a straight line but an average spectrum drawn through them gives an exponent of -1.6. The absolute intensities are more than a factor of ten down on the proton intensities.

Following their calculation of the proton spectrum Gloeckler and Jokipii have extended their differential helium spectrum up to an energy of 100 GeV / nucleon (Fig. 2.2). If a constant slope of -1.65 is assumed for the integral spectrum of helium nuclei above this energy then it is found to agree quite well with average spectrum of the three emulsion measurements described above (Fig. 2.4). This was not the case with the proton measurements where the intensities from emulsion data were a factor of three higher than the extrapolated spectrum of Gloeckler and Jokipii.

There are no measurements available on the helium spectrum above an energy of 10^{13} eV / nucleon.

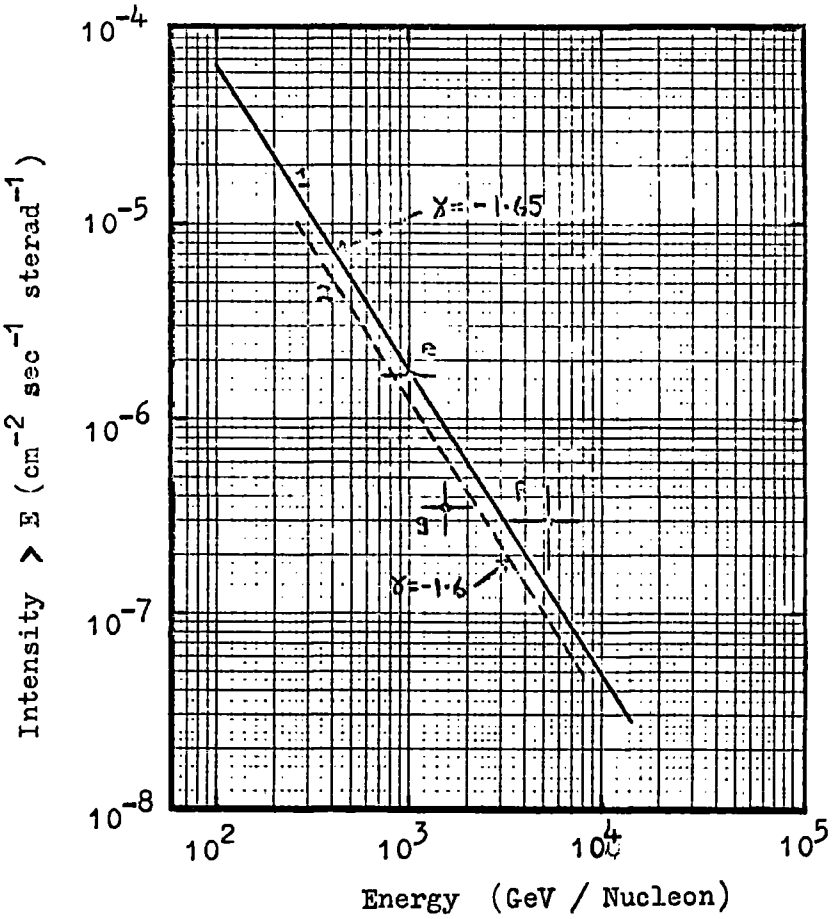

Figure 2.4 Integral Spectrum of Primary Helium Nuclei above 100 GeV / Nucleon.

e: Fowler and Waddington (1956).
f: Lohrmann and Teucher (1959).
g: Jain et al. (1959).
1: Extrapolation of Helium Spectrum given by Gloeckler and Jokipii (1967).
2: Average of experimental points.

2.5 Spectrum of Nuclei with $Z \geq 2$

These nuclei represent about two per cent of the total primary radiation intensity above a given rigidity. There are often large differences in intensity of the different charge components and so it has been found useful to divide the nuclei up into the following charge groups:

a) The L nuclei : Lithium, Beryllium and Boron, $3 \leq Z \leq 5$

b) The M nuclei : Carbon, Nitrogen, Oxygen and Fluorine $6 \leq Z \leq 9$

c) The H nuclei : Neon and heavier nuclei, $Z \geq 10$

M and H nuclei are often grouped together and called S nuclei.

This grouping is based on the astrophysical evidence that carbon, nitrogen and oxygen are cosmically the most abundant heavy elements while there is almost a total lack of lithium, beryllium and boron.

There are a number of difficulties involved in the measurements of the spectra of these nuclei especially those using balloons. Being heavy nuclei they have short interaction lengths in the atmosphere and after an interaction will produce elements of lower charge groups which will be indistinguishable from the primaries. Thus it is necessary to apply corrections for fragmentation that occurs in any overlying atmosphere. In the past the magnitude of these corrections has represented an important source of controversy on the estimate of the L nuclei flux at the top of the atmosphere and many problems in connection with the interpretation of the abundances of the various H nuclei as well.

2.5.1 Spectrum of S nuclei

Being the most abundant the S nuclei (M+H nuclei) are the easiest to measure. Fan et al (1967) have made satellite measurements on carbon, oxygen and nitrogen in the region 10-1000 MeV / nucleon (see Fig. 2.2). They find a spectrum whose shape is similar to that of protons and He nuclei but the intensities are a factor of over one hundred times less than the proton intensity. Carbon and oxygen appear to have about the same intensity but that of nitrogen is four times less. Webber (1967) summarises data which agrees with these spectral shapes although the spectra do not distinguish between the separate elements. At higher energies there is only one measurement on S nuclei. This is by Jain et al (1959) who used emulsions flown in a balloon. The intensity refers to an energy of 10^{11} eV / nucleon (Fig. 2.6) and is compatible with an He : S ratio that does not change with energy over the range of experimental measurements.

2.5.2 Spectrum of L nuclei

The spectrum of L nuclei is less well known. Webber (1967) gives a spectrum which exhibits a maximum at around 150 MeV / nucleon similar to that described for the proton and helium spectra. The intensities are a lot less than those of S nuclei. Fan et al. (1967) have measured the intensities of the individual components of the L nuclei over a small energy range. These are shown in Fig. 2.2 and it can be

seen that the spectra of lithium, beryllium and boron are tending to fall with increasing energy at about 60 MeV /nucleon which is contrary to the shapes of the proton, helium, carbon and oxygen spectra. Both Webber and Fan et al give an L : S ratio of about 0.23 at 100 MeV / nucleon and above while at lower energies the ratio appears to increase. Above 1 GeV / nucleon there are no direct measurements on L nuclei.

2.6 Primary Spectrum above 10^{14} eV / Nucleon

In this energy it is only possible to investigate the primary cosmic ray spectrum indirectly from extensive air shower information gained at or near sea level. A survey of these results has been given by Greisen (1965) and this is shown in Fig. 2.5. The main features of the spectrum are: in the region 10^{10} -10^{15} eV / nucleon the spectrum can be represented by a power law with exponent -1.6. From 10^{15} -10^{18} eV / nucleon the slope steepens to about 2.2 and then above 10^{18} eV / nucleon seems to flatten again to -1.6 although at these energies the information is very sparse as the rate of events is very small.

The change in slope of the primary spectrum was originally proposed to explain the observed altitude variation of the change in slope of the density spectrum of air showers. This variation might also be expected to show itself in the number spectrum, but while it seems well established that a change in slope occurs, it is by no means certain that the location of this change varies significantly with

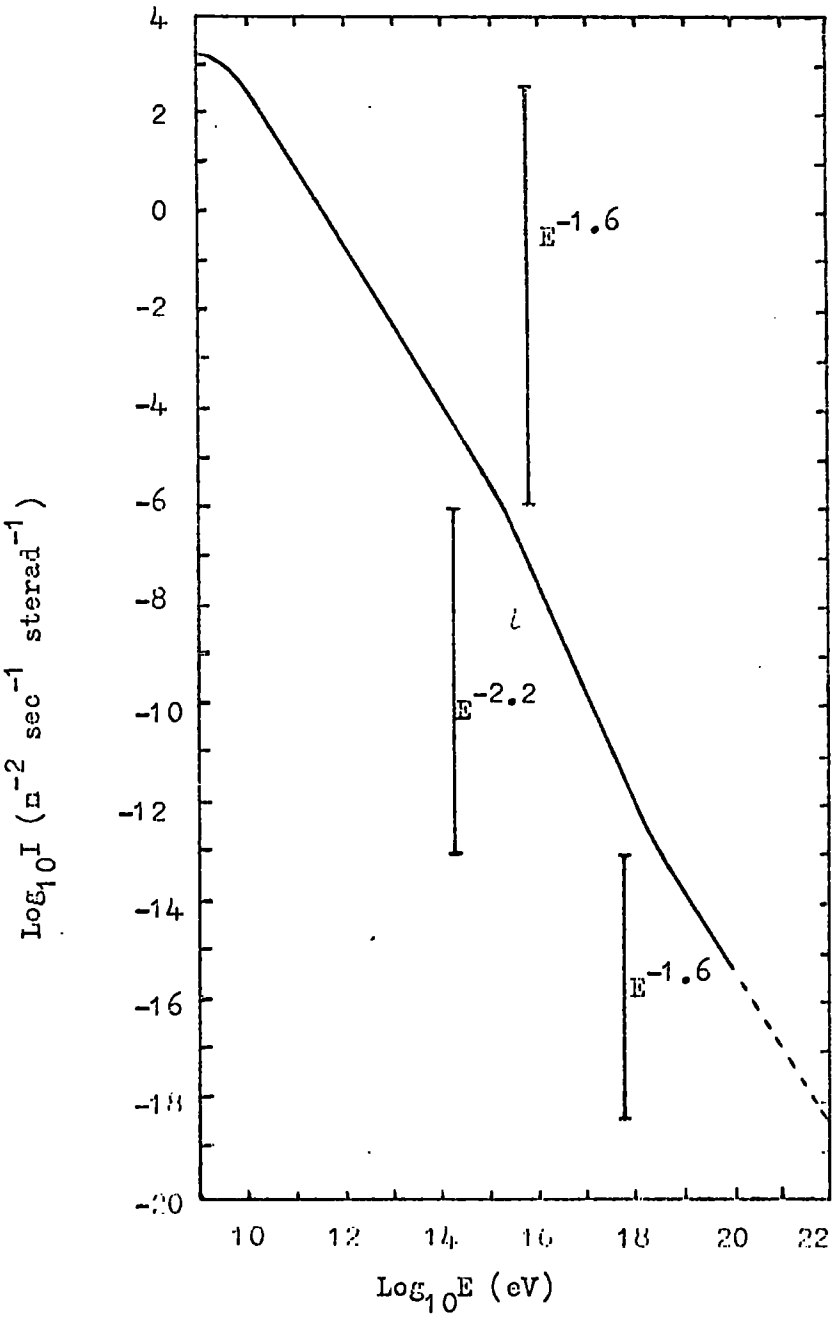

Figure 2.5 Integral Primary Cosmic Ray Spectrum after Greisen (1965).

altitude. Nikolskii (1967) doubts whether this behaviour can be explained solely in terms of a change in the primary spectrum and he proposes a new process which affects the interaction in the atmosphere leading to the shower. This process becomes important at about 4.10^{13} eV and transfers a large fraction of energy into the electron-photon component. While this can be used to explain the observed features of air shower densities it is not proposed that it is the only factor involved in the steepening of the density spectrum.

The primary spectrum one obtains from the air shower measurements depends to a large extent on the assumptions made regarding the interaction of the primary particles and the subsequent passage of the shower through the atmosphere. At the present time it would appear that there is considerable disagreement regarding the composition of the primary spectrum in these high energy regions.

2.7 Summary of the different charge groups in the energy range 10^{10} -10^{14} eV / nucleon

The relative abundance ratios of the different charge groups are best summarised in the following table (Table 2.1.) given by Webber (1967). This gives the ratios of the various charge groups as a function of rigidity etc. and refers to the energy range 10^{10} -10^{14} eV.

It is possible that some of these ratios stem from measurements that may be in error but it should be noted that they agree quite well with ratios measured in the energy range 3-30 GeV / nucleon. It would therefore appear that there is no reason to believe that in the range

3.10^9 - 10^{14} eV / nucleon any relative change in the spectra of the various groups occurs.

	Rigidity	Energy/Nucleon	Total Energy per Nucleus
P/He	6.4 ± 0.3	17.6 ± 1.2	4.4 ± 0.3
He/S	11.6 ± 0.2	11.6 ± 0.2	1.5 ± 0.03
L/S	0.26 ± 0.02	0.25 ± 0.02	0.08 ± 0.01
H/M	0.30 ± 0.02	0.30 ± 0.02	0.66 ± 0.04
P/Z⩾2	5.8 ± 0.3	16.0 ± 1.2	2.4 ± 0.2

Table 2.1 Relative abundance ratios of the different charge groups.

2.8 Primary Nucleon Spectrum in the energy range 10^{10} -10^{14} eV / nucleon

In making comparisons between the primary spectrum and the nucleon spectra at various depths in the atmosphere it is necessary to have a good estimate of the primary nucleon spectrum in the region where the exponent is constant. This is so in say the measurement of the nucleon attenuation length on its passage through the atmosphere. Nucleons are present in the primary particles in the form of single protons, and as protons and neutrons in the nuclei of heavier elements. In Fig. 2.6 are shown what are thought to be the best estimates of the spectra of

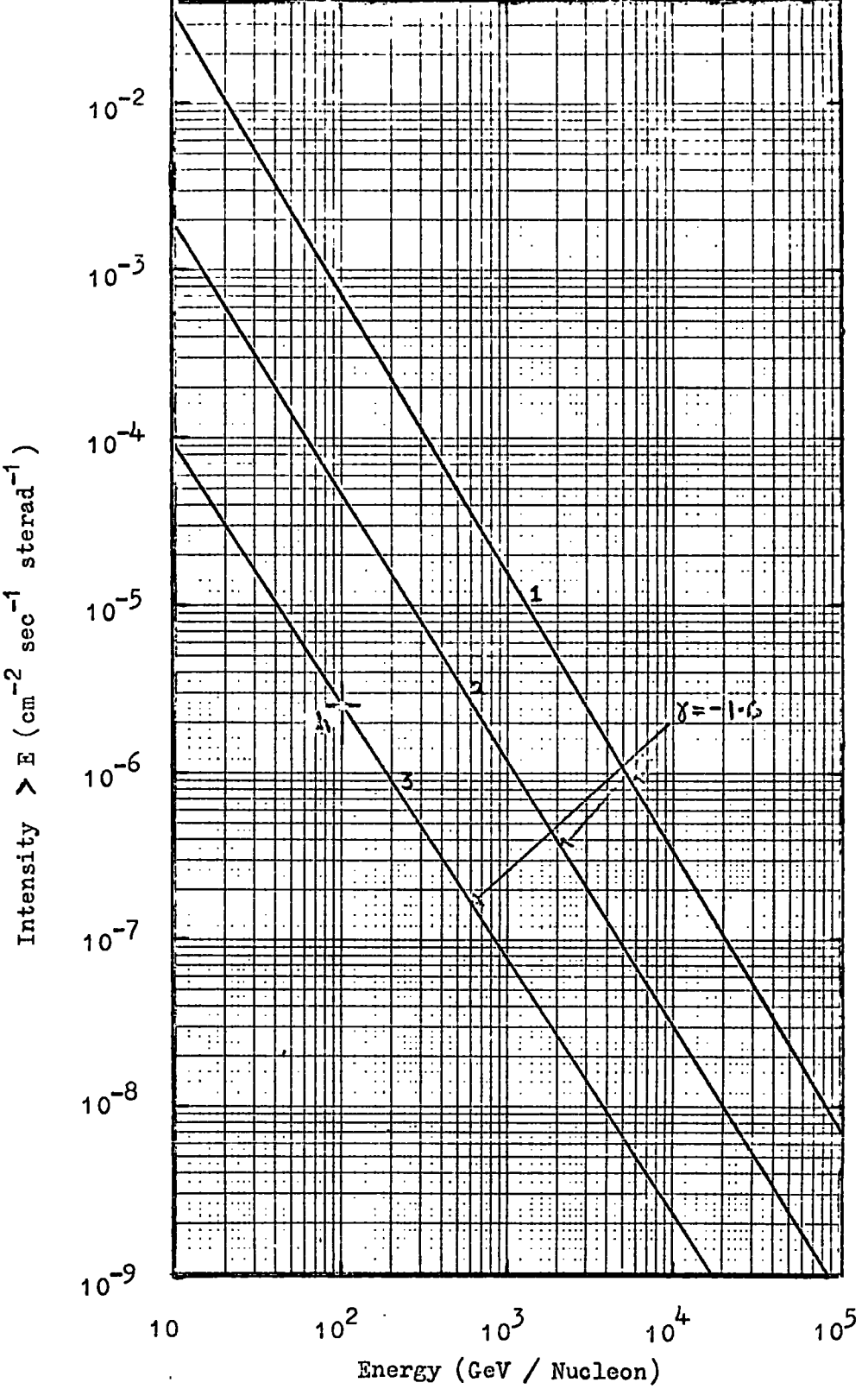

Figure 2.6 Spectra of the various Primary Charge Groups.

1: Protons 2: Helium Nuclei.
3: S Nuclei.
h: Jain (1959).

the various charge components in the primary radiation. The resulting spectra of protons and neutrons are shown in Fig. 2.7. This shows that protons are the main component.

In evaluating the nucleon spectrum it has been decided to adopt as the single proton spectrum an extension to the data of Gloeckler and Jokipii (1967). This spectrum is in good agreement with the low energy data and also with all the indirect determinations of the total radiation spectrum including those from air shower measurements at higher energies.

The helium spectrum used is the average line drawn through the three experimental points in the range 10^{11} - 10^{13} eV / nucleon. This spectrum is in good agreement with the data of Gloeckler and Jokipii and also gives a P : He ratio consistent with that at lower energies.

A line of slope -1.6 drawn through the point at 10^{11} eV / nucleon, Jain et al (1959), has been adopted for the spectrum of S nuclei. This gives intensities slightly lower than an extension to the data of Gloeckler and Jokipii but is in good agreement with the relative abundances of the various charge groups at lower energies. In calculating the contribution of S nuclei to the nucleon spectrum a mean Z of 8 has been used. This is the mean value of the M group which form the major part of the S nuclei.

The L nuclei are assumed to have intensities 0.23 times those of S nuclei. Their contribution to the nucleon spectrum is very small.

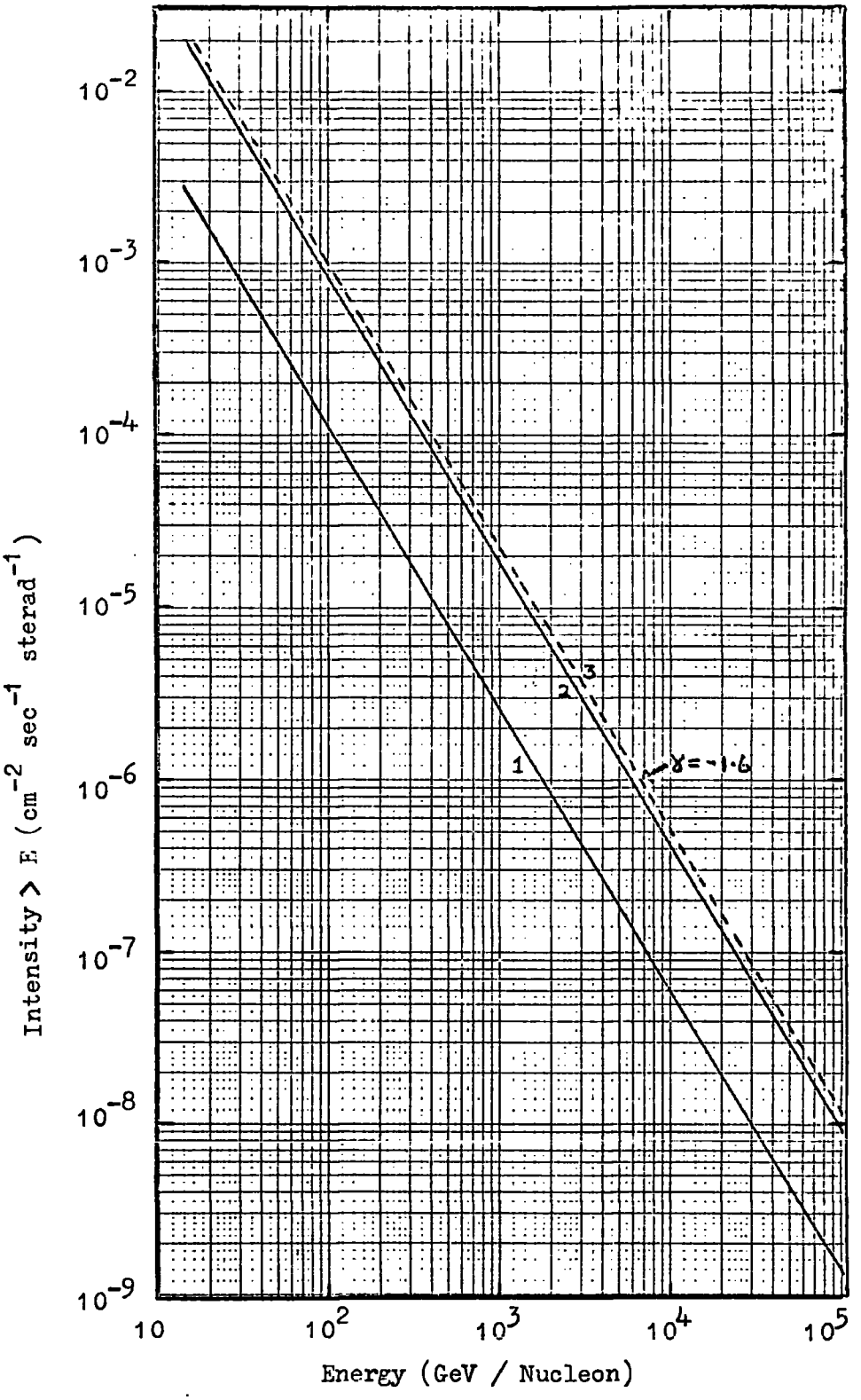

Figure 2.7 Integral Spectra of Primary Nucleons.

1. Neutrons. 2. Protons.
3. Nucleons (Protons + Neutrons).

2.9 Measurements from "Proton" Satellites

Results have now been presented from the Proton 1, Proton 2 and Proton 3 flights, Grigorov et al (1969). On all three flights the basic instrument was an ionisation calorimeter. The charge of incoming particles was measured by proportional counters and these particles then interacted in a thick target (carbon or polyethylene). The products of the interaction were absorbed in the ionisation calorimeter (a series of scintillators interleaved with iron absorber) which enabled the energy of the primary particle to be estimated.

Measurements were made of the spectrum of all particles irrespective of charge and that of protons alone. The results from each of the three flights have been analysed independently. Fig. 2.8 shows the integral spectrum of all particles in the energy range 5.10^{10} - 10^{14} eV and this can be approximated by a power law of the form $I\ (>E) = A\ E^{-(\gamma-1)}$ with $(\gamma-1) = 1.73 \pm 0.05$. This line is a best fit to the experimental points from all three flights which are in good agreement with each other.

Single protons were selected using the proportional counters. An additional aid in this respect on the Proton 3 flight was the use of a Cerenkov directional detector which enabled particles moving backwards from the calorimeter to the proportional counters to be detected. The resulting spectrum has an exponent $\gamma = 1.7$ at $E < 10^{12}$ eV and $\gamma \sim 2.5$ in the energy range 2.10^{12} - 10^{13} eV. The spectra obtained independently from the three flights including the one employing the directional detector are in agreement indicating that the steepening of the spectrum

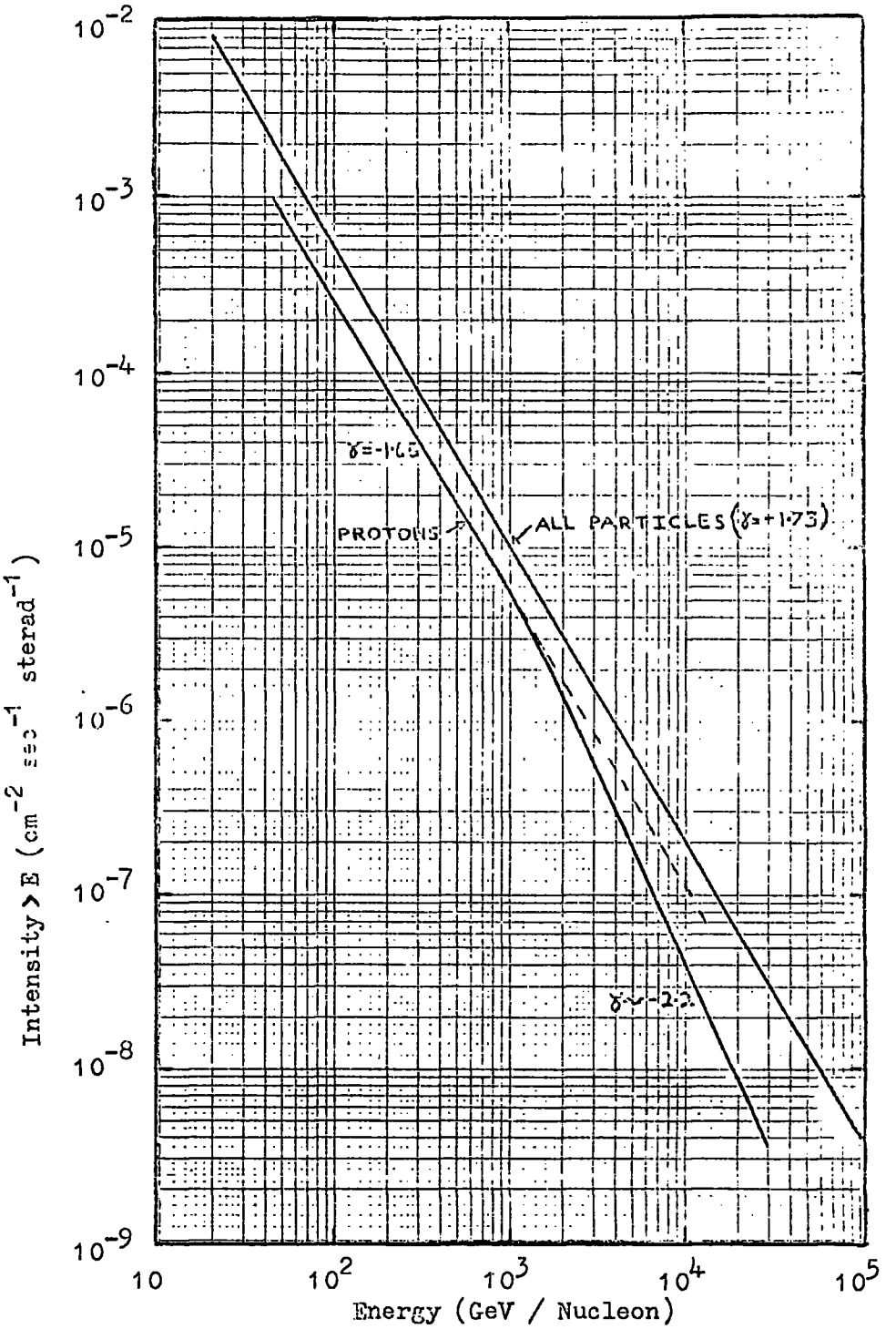

Figure 2.8 Primary Proton and All Particle Spectra From the "Proton" Satellite Measurements.

at 10^{12} eV cannot be attributed to backward moving particles from the calorimeter, Fig. 2.8 shows a best fit to the experimental points which is represented by the function.

$$I(\geq E) = 3.10^{4}\left(\frac{100}{E}\right)^{1.62} \times \frac{1}{\left[1 + \left(\frac{E}{1500}\right)^{2}\right]^{0.35}} \text{ cm}^{-2} \text{ sec}^{-1} \text{ sterad}^{-1}$$

with E in GeV.

It will be noted that the spectrum of all particles does not exhibit the change in slope shown by the protons only spectrum. It can be shown, however, by taking the above spectrum of protons together with a spectrum of bursts from nuclei with $Z \geq 2$ of the form

$$I_{g}(\geq E) = 3.10^{4}\left(\frac{100}{E}\right)^{1.62}$$

that the change in exponent of the proton spectrum does not contradict the observed spectrum of all particles i.e. the all particle integral spectrum can be represented by a single power law with exponent $(\gamma-1) = 1.73$.

2.10 Conclusions

The flux of primary cosmic ray protons and neutrons has been estimated from the spectra of the various charge components. The result is shown in Fig. 2.7 and this data is used further in Chapter 7 in interpreting the measured sea level neutron spectrum. The nucleon

spectrum shown in Fig. 2.7 is believed to be correct despite the fact that the recent measurements of Grigorov et al give a proton spectrum in disagreement with all previous determinations. The reason for this is that the apparatus of Grigorov et al contained no visual detectors and it is believed that backward moving particles could enter the charge measuring counters and cause protons to be recorded as α-particles etc. This effect could be responsible for the deficit of protons above 10^{12} eV.

CHAPTER 3

PROPAGATION OF NUCLEONS IN THE ATMOSPHERE

3.1 Introduction

Nucleons are known to exist in the primary cosmic rays in the form of single protons and as protons and neutrons in the heavier nuclei. The spectra of the various primary components have already been described in the previous chapter. On passing through the atmosphere these primary particles interact with the air nuclei. The heavier nuclei have relatively short interaction mean free paths and in their collisions fragment into nuclei of lower atomic number. Thus after a few interactions they have completely split into their constituent nucleons. Following their interactions with air nuclei the nucleons emerge with a certain fraction of their initial energy, the majority of the remainder going into the production of pions. Hence in the sea level flux of cosmic rays there will be a certain contribution from protons and from neutrons. The primary spectrum is fairly well established at least up to energies of the order of 10^{14}eV while at sea level the muon spectrum has been measured to beyond 10^{12} eV and that of protons to around 10^{11} eV. These primary and sea level spectra are interrelated so that by adopting a propogation model it is possible to draw certain conclusions relating to the interactions of nucleons in the atmosphere. For example, it will be seen that the neutron to proton ratio at sea level depends on the

value of the charge exchange probability in nucleon collisions.

3.2 Interaction Cross-sections and Mean Free Paths of Nucleons

Measurements of the elementary nucleon-nucleon inelastic cross-section have been performed using accelerators up to energies of a few tens of GeV. Above these energies the cross-sections have to be determined in cosmic ray experiments and these results extend up to 100 GeV and over. When, as in the accelerator experiments, the measurements are performed using hydrogen bubble chamber targets the nucleon-nucleon cross-section can be obtained directly. In cosmic ray experiments, however, the targets are usually composed of heavier elements such as iron or carbon so the parameter measured is the nucleon-nucleus cross-section. Thus it is important to have a relationship between the elementary particle-nucleon and the particle-nucleus cross-section.

In the first approximation this can be calculated as in Rossi (1952). At high energies the interaction is considered to be between the incident particle and the individual nucleons of the target nucleus. According to this description an inelastic collision occurs when the incident particle, on traversing the nucleus, interacts with at least one of its nucleons. The probability of this event occurring depends on the cross-section σ for particle-nucleon collisions. It is assumed that the nucleons are distributed at random in a sphere of radius r. Considering a particle at a distance b from the centre of the nucleus there will

be a certain volume swept out by its cross-section σ as it traverses this nucleus. The size of this volume denoted by Ω will depend on the impact parameter b, the nuclear radius r and σ. According to Poissonian statistics the probability that no nucleons are present in Ω is given by exp $(-\Omega A/V)$ where A is the atomic weight and V the volume of the nucleus. Then the total cross-section for an inelastic collision of the elementary particle with the nucleus is

$$\sigma_i = \int_0^{r+r_1} 2\pi \left[1-\exp\left(-\frac{\Omega A}{V}\right)\right] bdb$$

where $\left[1-\exp(-\Omega A/V)\right]$ is the probability that an interaction occurs when the impact parameter is b and r_1 is the radius of interaction of the primary particle given by $\pi r_1^2 = \sigma$.

In practice, however, electron-nucleus scattering experiments [e.g. Hofstadter (1959)] have shown that the nuclei are not spheres of constant density. These experiments yield the charge distributions for different nuclei and it has been shown by Brenner et al (1957) and Abashian et al. (1956) that the density of nucleons in the nucleus is proportional to the density of charge. Using the charge distributions obtained from these experiments it is possible to evaluate the nucleon-nucleus cross-section as a function of σ in a more exact way. This has been done by Williams (1960), Brenner et al (1957), Alexander et al (1961) and Bozoki et al (1961) for various materials. In Fig. 3.1. are shown the calculated points for air nuclei as these are relevant

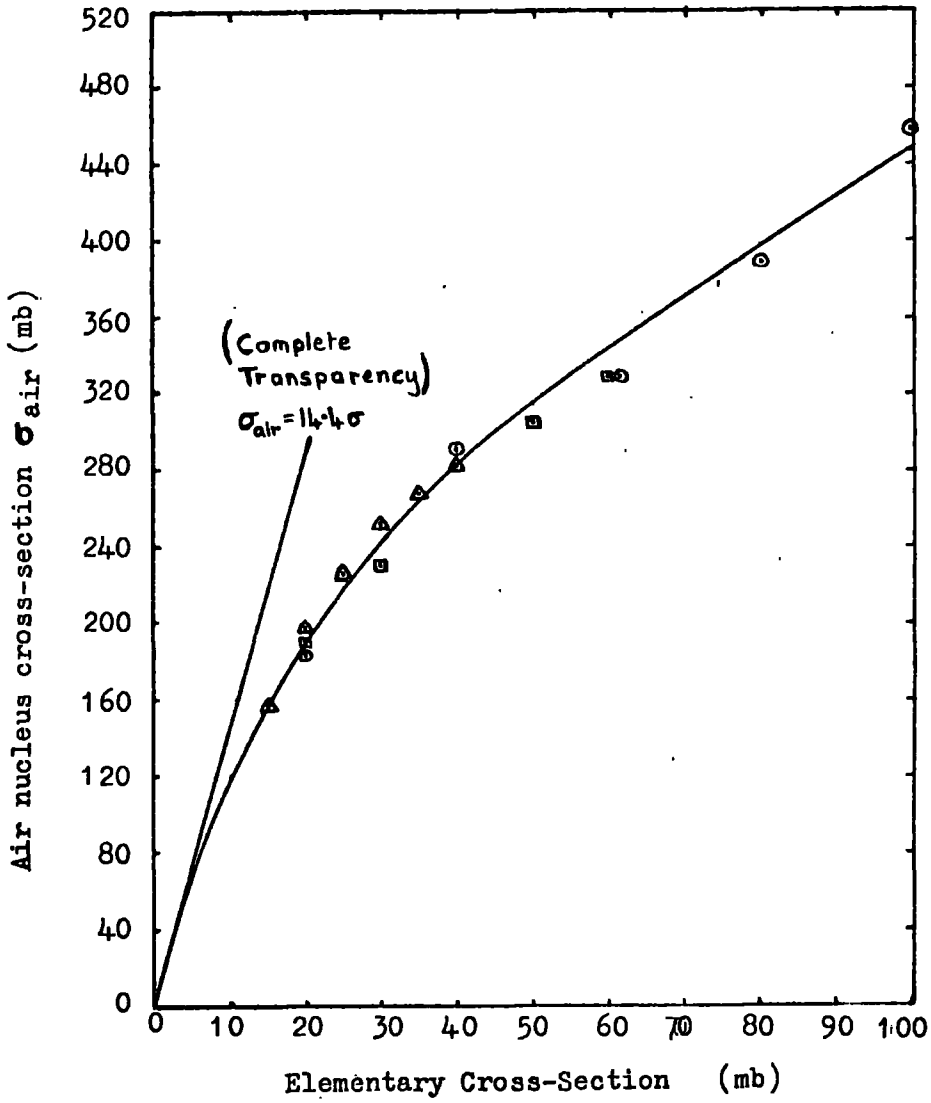

Figure 3.1 Average air nucleus cross-sections as a function of the elementary cross-section.

- Alexander et al (1961).
- Williams (1960).
- Constant density spheres, $r = 1.38.10^{-13} A^{\frac{1}{3}}$ cm.

to nucleon interactions in the atmosphere. The exact calculations can be compared with the more approximate method in which the points have been evaluated assuming that nuclei are spheres of constant density with radius $1.38.\ 10^{-13}\ A^{1/3}$ cms. There is seen to be reasonable agreement between the two over the common region of σ i.e. 20-60 mb. Hofstadter (1957) gives the radius of the equivalent sphere for oxygen as $1.35.\ 10^{-13}\ A^{1/3}$ and the closeness of 1.38 to 1.35 is the reason for the agreement.

Thus having established a means of determining the relationship between the nucleon-nucleus and elementary nucleon-nucleon cross-section σ it is possible to measure σ from experiments using heavy targets. A summary of the experimental data up to energies in excess of 100 GeV is shown in Fig. 3.2. It will be seen from this that the elementary inelastic cross-section rises from zero at a nucleon kinetic energy of 350 MeV to about 30 mb at just greater than 1 GeV. Above this energy the points seem to lie in the region of 30 mb although there is evidence for a rise in the cross-section above 100 GeV from the "Proton" satellite measurements, Grigorov et al (1969).

Now that a reasonable estimate of the elementary nucleon-nucleon cross-section and the relationship between it and the nucleon-nucleus cross-section have been established it is possible to evaluate the latter quantity and hence the interaction length of nucleons in various materials. The transparency curve for air which is the relevant medium here has already been given in Fig. 3.1. The interaction length

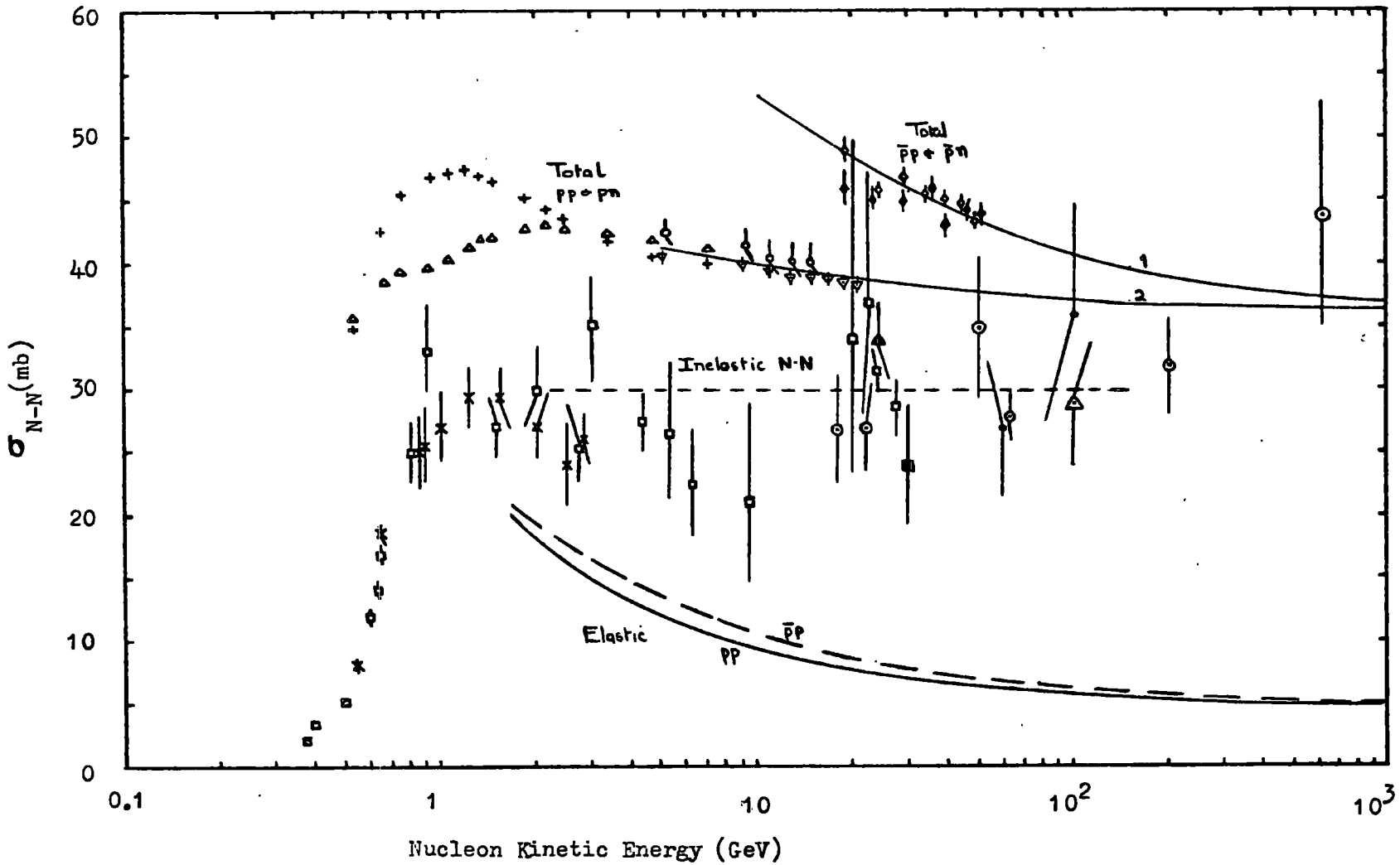

Figure 3.2 Summary of the Experimental Measurements of the Total and Inelastic N-N Cross-Section. (Caption on next page).

CAPTION TO FIGURE 3.2

1. Experimental Measurements of the Inelastic N-N Cross-Section

- ⏢ Alakoz et al (1967)
- ■ Bozoki et al (1961)
- • Bozoki et al (1967)
- ▲ Cocconi (1961)
- ⊙ Grigorov et al (1967)
- □ Jabs (1967)
- × Lindenbaum (1957)

2. Experimental Measurements of the Total Cross-Section

- ◇ $\bar{p}p$, ◆ $\bar{p}n$ } Allaby et al (1969)
- + pp, △ pn } Bugg et al (1966)
- ▽ pp, ○ pn } Galbraith et al (1965)

The Theoretical Curves 1 and 2 represent the total cross-sections for $\bar{p}p$ and pp respectively calculated from a Regge Pole Model, Barger et al (1968). The curves for the pp and $\bar{p}p$ elastic cross-section are from the same authors.

It will be seen the total and elastic pp cross-sections up to 1000 GeV are consistent with an inelastic p-p cross-section of 30 mb. This is contrary to the findings of Grigorov et al (1969) but in agreement with the general trend of other experimental results.

can be evaluated from the expression $\lambda_{int} = A/N\sigma_i$ where A is the atomic weight of the material, N is Avagadro's number and σ_i the inelastic cross-section in the given material. Thus for air this becomes

$$\lambda_{int} = \frac{14.4}{6.10^{23}.\sigma_{air}} = \frac{2.4.10^{-23}}{\sigma_{air}}$$

Hence it is possible to evaluate a relationship between the interaction length in air and the elementary nucleon-nucleon cross-section σ. This is shown in Fig. 3.3. The results of different sets of calculations are again shown and there is seen to be a very good agreement.

It will be seen from this curve that an elementary nucleon-nucleon cross-section of 30 mb (the value about which the experimental points on Fig.3.3 appear to lie above an energy of 1 GeV) corresponds to a nucleon interaction length in air of 96 gm.cm.$^{-2}$. In the past the attenuation length of nucleons in the atmosphere has generally been accepted as being in the region of 125 gm.cm.$^{-2}$ the difference between it and the interaction length being due to the nucleon elasticity. However, a value of λ_i in the region of 90-100gm.cm.$^{-2}$ which seems reasonable from Fig.3.3 leads to less elasticity than is normally assumed. This arises from the fact that in the past it has been assumed that at very high energies the inelastic nucleon-nucleon cross-section approaches the total cross-section but Fig. 3.2 shows

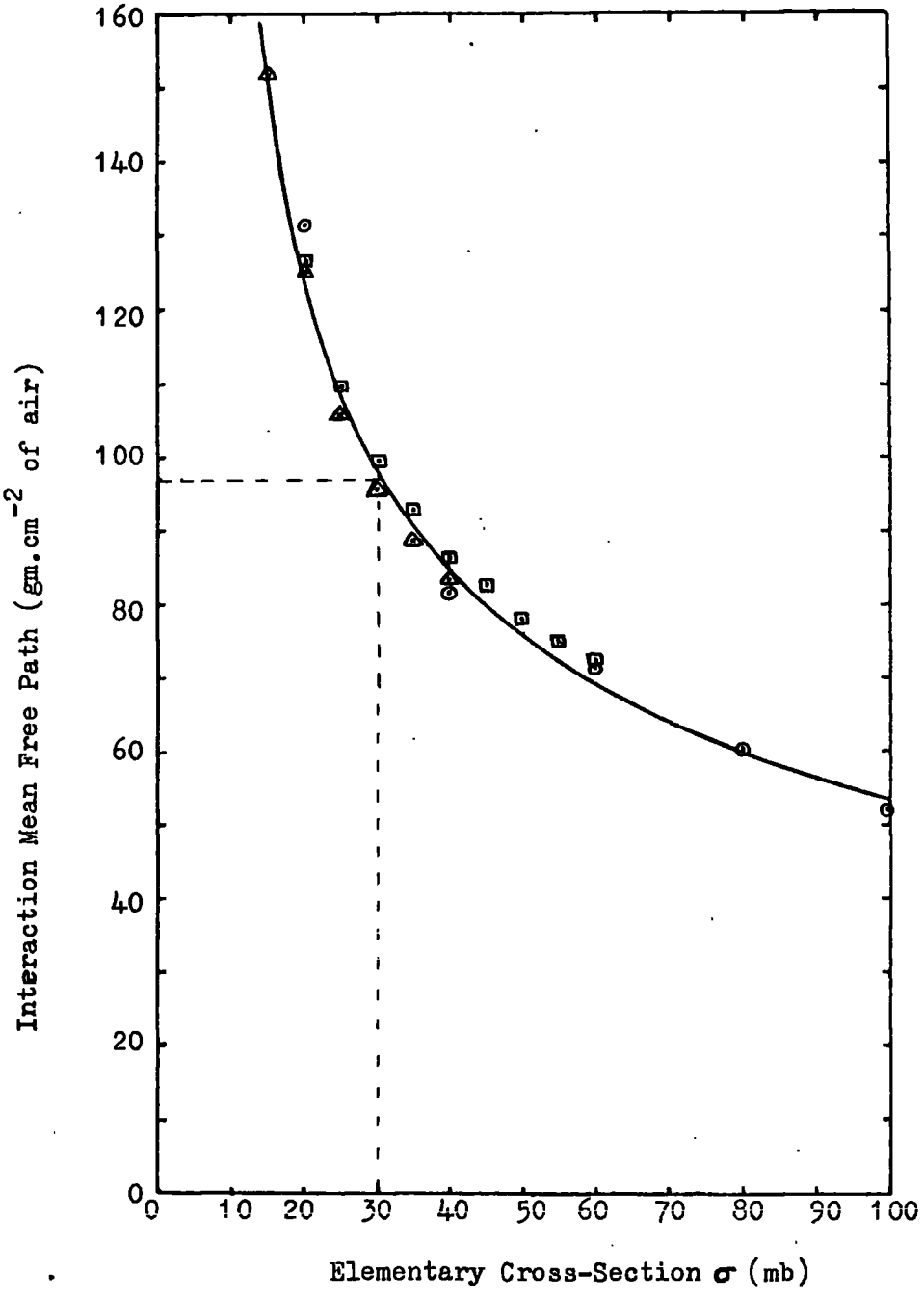

Figure 3.3 Interaction Mean Free Path in air as a function of the Elementary Cross-Section.

- ◻ Alexander et al (1961).
- △ Williams (1960).
- ⊙ Constant density spheres, $r=1.38.10^{-13}A^{\frac{1}{3}}$ cm.

that this is still falling at 20 GeV so it is difficult to estimate at what value they would meet. There is also no definite direct experimental evidence to support this.

Where it is required in the present work a value of $\lambda_i = 96 \text{gm.cm.}^{-2}$ has been assumed.

3.3 Energy Spectrum of Nucleons in the Atmosphere

It is generally supposed that the primary differential nucleon spectrum can be expressed in the form $N(E_p)dE_p = AE^{-\gamma} dE_p$ at least in the energy range $10^{10} - 10^{15}$ eV. On passing through the atmosphere the nucleons interact with the air nuclei and in each interaction they will on the average retain a certain fraction β of their energy. Thus after r collisions a nucleon of primary energy E_p will have an energy $E = \beta^r E_p$. If the mean free path for interaction of the nucleons with air nuclei is λ then the average number of collisions made by a nucleon in an atmospheric thickness t is $m = t/\lambda$. The probability of a nucleon making r collisions in this depth is $P(r) = e^{-m} m^r/r!$ Thus the differential energy spectrum of nucleons at a depth t is given by

$$N(E)dE = \sum_{r=0}^{\infty} A\left(\frac{E}{\beta^r}\right)^{-\gamma} \frac{dE}{\beta^r} P(r)$$

Substituting for P(r) gives

$$N(E)dE = \sum_{r=0}^{\infty} AE^{-\gamma}\, \beta^{r\gamma}\, \frac{dE}{\beta^{r}} \cdot \frac{e^{-m} m^{r}}{r!}$$

$$= AE^{-\gamma}\, dE\, e^{-m} \sum_{r=0}^{\infty} \frac{\beta^{r(\gamma-1)}\, m^{r}}{r!}$$

Evaluating the summation and putting $m = t/\lambda$ gives

$$N(E)dE = AE^{-\gamma}\, dE\, e^{-(t/\lambda)(1-\beta^{(\gamma-1)})}$$

which can be written

$$N(E)dE = Ae^{-\left[\frac{t}{\lambda/(1-\beta^{(\gamma-1)})}\right]} E^{-\gamma}\, dE.$$

Thus under these conditions the differential energy spectrum of nucleons at a depth t is the same as the primary spectrum except that the intensity is reduced by a factor

$$e^{-\left[\frac{t}{\lambda/(1-\beta^{(\gamma-1)})}\right]}.$$

The quantity $\lambda/(1-\beta^{(\gamma-1)})$ is called the attenuation length λ_p. Values of λ_p evaluated using this relation are shown in Table 3.1 assuming $(\gamma-1) = 1.6$. The value of λ_p can be estimated from the zenith angle distributions of nucleons and the interaction length λ has been calculated in 3.2 so the elasticity β can be determined.

β	λ = 70g.cm^{-2}	λ = 80g.cm^{-2}	λ = 90g.cm^{-2}	λ = 100g.cm^{-2}
0.3	82	93	105	117
0.4	91	104	116	130
0.5	104	119	134	149
0.6	125	143	160	179
0.7	160	183	205	230

Table 3.1 Attenuation length λ_p as a function of interaction length λ and nucleon elasticity β .

3.4 Neutron : Proton Ratio in the Atmosphere

The target nuclei in the atmosphere contain equal numbers of protons and neutrons. If the incident cosmic ray beam were also charge symmetric then all secondary components of cosmic radiation would have to exhibit charge symmetry on any model of particle creation. In actual fact the primary cosmic ray particles bring a known amount of excess positive charge and the manner in which this excess is shared by the various secondary components of cosmic radiation provides clues to the nature of high energy interactions.

The neutron to proton ratio has been considered from a theoretical point of view by Yash Pal and Peters (1964). If the probability that a nucleon after colliding with a charge symmetric target and after possible excitation and decay emerges in a different charge state is represented by w then after j collisions the original composition of

the nucleon beam δ_o will be changed to

$$\delta_j = \left(\frac{p-n}{p+n}\right)_j = \delta_o (1-2w)^j$$

where $\delta_o = \frac{p_o-n_o}{p_o+n_o} = 0.77$ (from Fig. 2.7).

At any depth x

$$\delta_x = \frac{N_p-N_n}{N} = \delta_o e^{-x\left(\frac{1}{\lambda} - \frac{1}{\lambda_p}\right)} \sum_{j=0}^{\infty} \left[\frac{x\beta^{(\gamma-1)}}{\lambda}\right]^j \frac{(1-2w)^j}{j!}$$

$$= \delta_o e^{\frac{-2x}{\lambda}} \left\langle \beta^{(\gamma-1)_w} \right\rangle$$

This quantity has been evaluated for various values of interaction length λ and the resulting neutron to proton ratios at sea level are shown as a function of the charge exchange probability w in Fig. 3.4 taking $\beta = 0.5$ and $(\gamma-1) = 1.6$. The expected fluxes of protons and neutrons at sea level are then given by

$$N_p(x,E) = N(0,E)\ e^{-x/\lambda_p} \cdot \left(\frac{1+\delta_x}{2}\right)$$

$$N_n(x,E) = N(0,E)\ e^{-x/\lambda_p} \cdot \left(\frac{1-\delta_x}{2}\right)$$

Thus for small values of δ_x which occur for values of $w \geq 0.4$ it is expected that the fluxes of neutrons and protons at sea level will be the same.

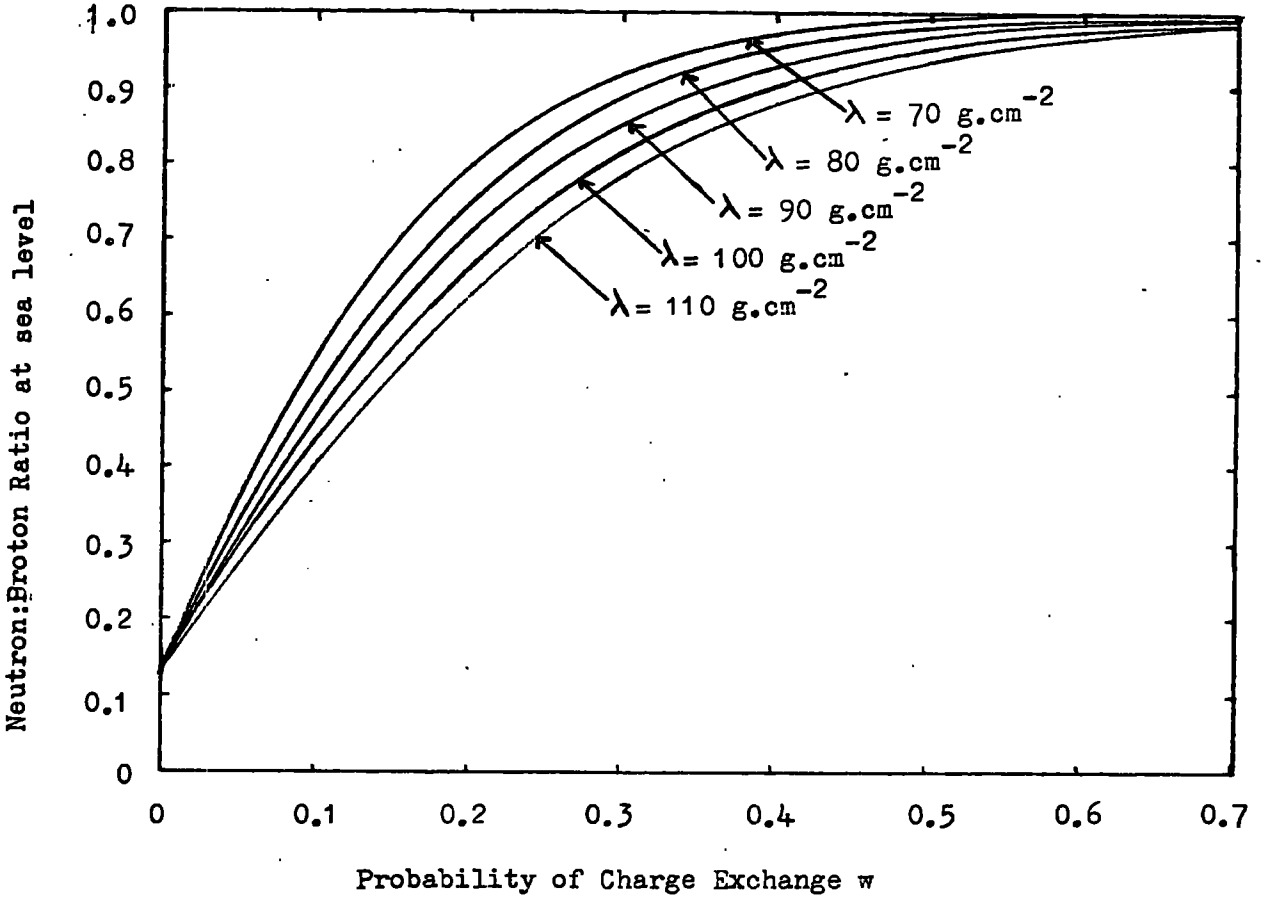

Figure 3.4 Neutron : Proton Ratio at sea level as a function of the Charge Exchange Probability w and the Interaction Length λ.

An experimental determination of the neutron to proton ratio has been made by Lal et al. (1963) at an atmospheric depth of 800 gm.cm^{-2}. The arrangement comprised a multiplate cloud chamber with an air Cerenkov counter above and a total absorption spectrometer below. The Cerenkov counter was used to distinguish pions from protons in the energy range 20-40 GeV and the accuracy of the energy determination from the total absorption spectrometer for individual events was estimated to be $\pm$ 20%. In the energy range 20-40 GeV the value of the neutron to proton ratio was found to be 0.98 $\pm$ 0.18. In Table 3.2 are shown their expected theoretical values of this parameter at 800 gm.cm^{-2} for different values of λ and w.

w	Expected N/P ratio at 800 gm.cm^{-2}.			
	λ =72g.cm^{-2}	λ=80g.cm^{-2}	λ=85g.cm^{-2}	λ =90g.cm^{-2}
0.5	0.98 (0.99)	0.94	0.87	0.80
0.4	0.94 (0.96)	0.88	0.80	0.71
0.3	0.87 (0.89)	0.78	0.68	0.58
0.2	0.71 (0.79)	0.60	0.50	0.43

Table 3.2 Expected values of N/P ratio at 800 gm.cm^{-2} according to Lal et al (1963) as a function of w and λ.

The figures in brackets give the ratio calculated taking into account the presence of heavy nuclei in the primary radiation (86% protons and 14% neutrons). All other figures are for protons only.

The neutron to proton ratios at 800 gm.cm^{-2} according to the expression given by Yash Pal and Peters are given in Table 3.3. These assume a primary composition as given in Fig. 2.7.

w	Expected N/P ratio at 800 gm.cm^{-2}.			
	λ=72g.cm^{-2}	λ=80g.cm^{-2}	λ=85g.cm^{-2}	λ=90g.cm^{-2}
0.5	0.96	0.94	0.93	0.92
0.4	0.92	0.89	0.88	0.86
0.3	0.83	0.80	0.79	0.76
0.2	0.70	0.65	0.63	0.61

Table 3.3 Expected values of N/P ratio of 800 gm.cm^{-2} according to expression of Yash Pal and Peters (1964) as a function of w and λ.

There can be seen to be some difference between the two sets of figures, one reason for this being the fact that those in Table 3.3 are calculated taking into account the presence of neutrons in the primary radiation while those of Table 3.2. are derived assuming protons only.

Lal et al conclude from their measured neutron to proton ratio of 0.98 $\pm$ 0.18 that there is an upper limit of 80% for the probability of charge persistence of nucleons in collision with air nuclei at energies in the region of 100 GeV.

3.5 Conclusions

Results of measurements of the inelastic nucleon-nucleon cross-section show its value to be approximately 30 mb in the energy range 1-100 GeV. Using experimental determinations of the charge distribution in nuclei the nucleon-nucleus cross-section can then be evaluated. These yield an interaction length in air for nucleons of 96 $gm.cm^{-2}$.

Estimates of the neutron to proton ratio as a function of the charge exchange probability w have been made and it is expected that there will be approximately equal fluxes of both at sea level for w in the range 0.4 - 0.5.

CHAPTER 4

REVIEW OF MEASUREMENTS OF NUCLEAR ACTIVE PARTICLES IN THE ATMOSPHERE

4.1 Introduction

The majority of experiments to study the interactions of nuclear active particles in the atmosphere have been performed at mountain altitudes although some measurements have been performed at sea level. The main reason for this is that the higher the altitude of the apparatus the greater the flux of high energy particles.

In theory cosmic rays can be studied at any depth in the atmosphere and the energy spectra of the different components measured. These components can be divided into two categories : (a) the nuclear active particles namely nucleons, pions, kaons and antinucleons and (b) muons. It is relatively simple to separate the muons from the strongly interacting hadrons of the same momentum but it is much more difficult to distinguish between say charged pions and protons at energies above 100 GeV. In the primary cosmic radiation protons represent about 85% of the particles the remainder being heavier nuclei so that the neutrons, pions and kaons must be secondaries produced in the nuclear interactions of the primaries while protons may be surviving primaries or secondaries. The energy spectra of all the different components are thus interrelated and depend on the characteristics of hadronic interactions at high energy. Therefore

by measuring the intensities of nuclear active particles at different depths in the atmosphere it is possible to obtain information about the nature of their interactions.

In this chapter measurements of the nuclear active spectrum at various depths in the atmosphere are summarised and compared. Unfortunately experiments at similar altitudes but using different techniques often give differing spectrawith the result that comparisons are hard to make.

4.2 Method of Measurement

The techniques used vary widely in detail but all utilise the characteristic strong absorption of the nuclear active particles to distinguish them from muons and soft components. The methods of energy measurement also differ considerably according to the range involved as does the accuracy of its determination. The established techniques can be divided into three categories:

a) direct measurements of parameters of the particle and its motion, for example its momentum or velocity.

b) measurements of some characteristic or characteristics of the nuclear interaction of the particles which depend in a known manner on its energy.

c) calorimetric methods.

Of these the first is only applicable up to energies of the order of a few hundred GeV. Typical examples within this category are the

measurement of energy from observations of the multiple scattering of a particle in a nuclear emulsion or from the curvature of the particle trajectory in a magnetic field. These methods are therefore only suitable for measurements of charged particles but for the energy range quoted earlier they can lead to reliable estimates of the particle energy.

The magnetic spectrometer technique gives a particularly reliable estimate of the particle momentum and in principle it should be possible with higher fields to measure higher energies. However, at larger energies larger apertures are required in order to record a reasonable rate of particles and it is not economic to construct magnets of the required dimensions.

Methods in category (b) have been developed and used in the region of energies $\gtrsim 10^{10}$ eV and they apply equally well for charged and uncharged particles. The method which has been used most frequently in the past is that developed by Castagnoli et al (1953) in which the kinematic characteristics of the interaction are employed. The method relies on a possible correlation between the angles of particle emission and the energy determination is rather unreliable.

Alternatively the electron-photon shower which eventually develops as the result of a high energy nuclear interaction can be studied and used as a basis for the determination of the primary energy. The straggling of the energy in these methods is quite considerable, however, for the relative proportions of energy transferred to photons

and to charged pions fluctuate strongly. This type of experiment is thus not very reliable for determining the energy of individual events but it can be employed more usefully in the measurement of a spectrum where a large number of events are being dealt with.

In general any characteristic of the elementary event which is energy dependent is subject to large fluctuations so that this category has only a limited application in the unique determination of particle energies.

The third category is the ionisation calorimeter. This was originally developed by Grigorov et al (1958) and initially it was intended for use in measuring the energy of individual particles, either charged or uncharged, in the energy range above 10^{11} eV. Subsequently the instrument has found much wider application and it has been used to study the processes and characteristics of high energy nuclear interactions, sometimes in combination with other apparatus such as the cloud chamber and nuclear emulsions. Briefly the principle behind the measurement of energy in the ionisation calorimeter is as follows. At the top of the instrument there is usually a large block of absorber in which the nuclear active particle interacts. Pions and hence photons are produced so an electron-photon cascade is initiated. This shower is allowed to develop in a series of thin absorbers and detectors and all the energy of the primary particle is absorbed. The calorimeter gives an electrical signal which is proportional to the energy absorbed. Generally these instruments

contain about seven interaction lengths of iron absorber and the cascade is usually sampled at more than six depths with scintillation counters or ionisation chambers. These devices can measure the energy of an individual particle to an accuracy of approximately 30% and so are a very great asset in the measurement of the flux of nuclear active particles. The measurement itself is sometimes complicated because of the presence of side showers. Also the instruments cannot be calibrated with artificially produced particles of known energy at the energy at which they are to be operated. Thus it is necessary to rely on cascade theory in the energy determination. In general the accuracy with which the energy is determined is dependent on:

i) the total thickness of the calorimeter

ii) the number of sampling counters.

The resolution attained may be as poor as $\pm$ 300% or as good as $\pm$ 15% so obviously the instruments differ widely. The associated shower detecting arrays are also different from experiment to experiment and this is another factor which makes the comparison of nuclear active energy spectrum from different atmospheric depths very difficult.

4.3 Measurements at $\sim$ 550 gm.cm^{-2}.

4.3.1 Kamata et al (1967)

This experiment, performed at an altitude of 5200 metres above sea level, consisted of a shielded 60m^2 scintillation counter detector

in the centre of the Chacaltaya air shower array. It was used to observe large bursts of size greater than 3000 particles which had been produced mainly by the interactions of nuclear-active particles of energy greater than 3.10^{12} eV in the absorber above the scintillator. The majority of these bursts were accompanied by extensive air showers which were detected by the BASJE array but some of the events were unaccompanied and these were considered to be due to residual primary nucleons.

Briefly the experiment consisted of a large array of shielded scintillation counters above which were five unshielded scintillators. The selection requirement was a coincidence between one of the unshielded counters and one of the shielded counters directly underneath it. This system acted as a vertical telescope with an acceptance aperture of 0.3 sterad. For unaccompanied events the selection requirements were that only one particle passed through the top unshielded counter and produced a large burst in the shielding material which was subsequently detected by the shielded counters. The energy of the burst producing particle was estimated from Monte Carlo calculations. It was assumed that all these single particles were surviving primaries. However, it is possible that they could already have produced a small shower in the upper atmosphere which had died out before it reached the apparatus. Thus the observed intensity of single particles detected by this experiment is understood to be an upper limit to the flux of residual primary nucleons at 5200 m.

The experimental points are shown in Figure 4.1. Assuming a primary nucleon spectrum of the form shown it can be seen that the observed intensities are consistent with an interaction length in air of between 80 gm.cm^{-2} and 90 gm.cm^{-2}.

Observations also showed that 99% of all large bursts were accompanied by extensive air showers of various sizes and arrival directions. Besides the shielded detectors there were 25 scintillation counters and five Cerenkov counters located at various distances from the centre of the array. The single unaccompanied event was such that, except for the coincidence counter, all the unshielded detectors recorded no particles.

More recent results presented by this group at the Budapest Conference (1969) indicate that the spectrum of surviving primary protons at this depth cannot have an exponent which is less than 2.0.

4.3.2 Akashi et al (1967) (Japanese and Brazilian Emulsion Chamber Group)

This was an experiment performed to study extremely high energy nuclear interactions using an emulsion chamber. The apparatus was situated at Mount Chacaltaya (altitude 5200 metres above sea level) and consisted essentially of three sections, namely the upper chamber, producing layer, and lower chamber respectively. The upper chamber which was composed of 8-cm lead plates and four nuclear emulsion layers was used to observe particles (mainly high energy γ-rays and electrons) coming directly from the atmosphere. The centre section was the jet

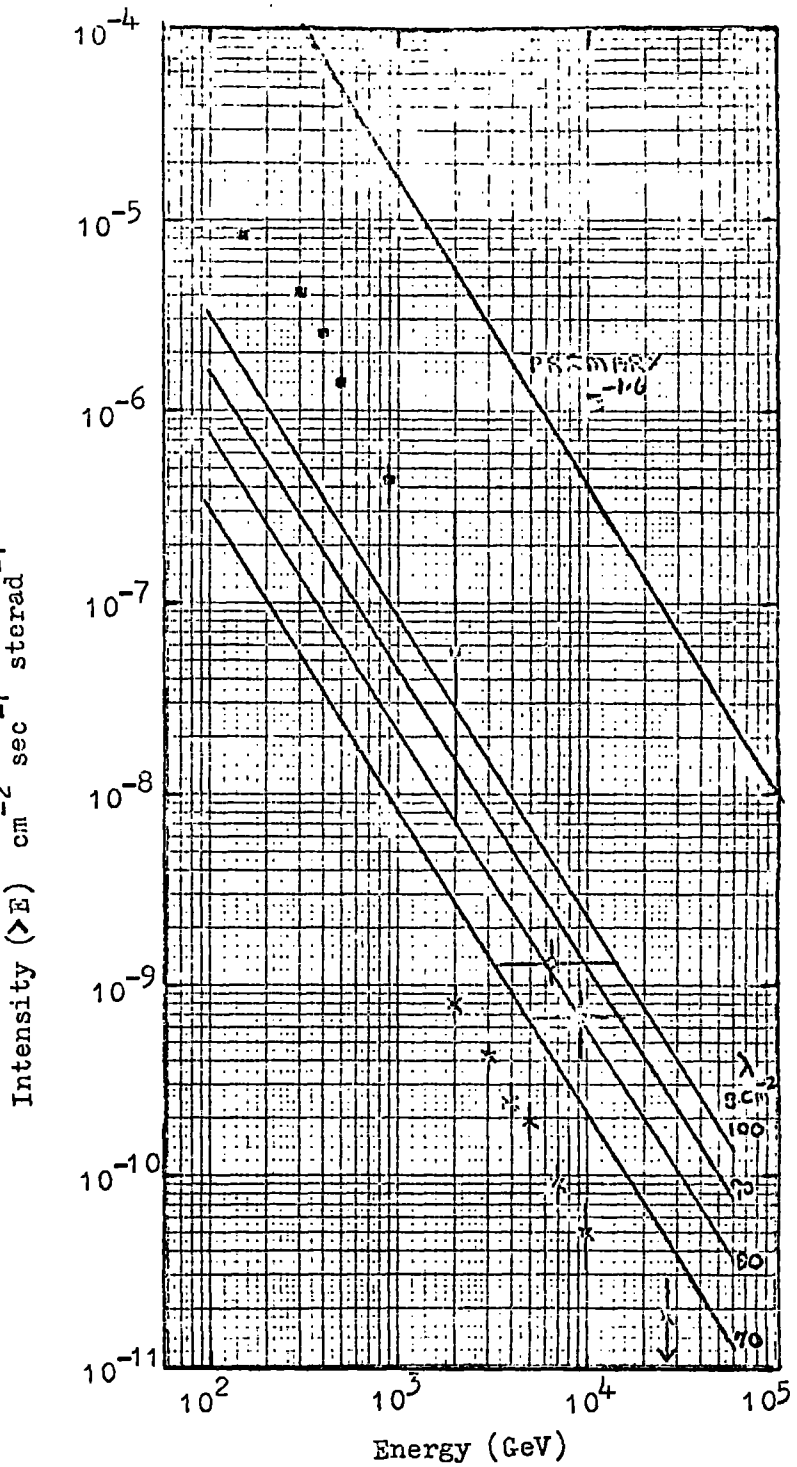

Figure 4.1 Flux of Nuclear Active Particles at $\sim$ 550 gm.cm^{-2}.

- ▪ Baradzei et al (1963).
- ∘ Kamata et al (1967).
- × Akashi et al (1967).

producing layer and was situated just below the upper chamber. This was made of 70 $gm.cm^{-2}$ of petroleum pitch. The lower chamber consisted of 20-cm lead plates and 13 emulsion layers.

Events detected in the lower chamber were selected for further measurement if the incident interacting particles passed through the upper chamber. These events were mainly nuclear interactions caused either in the producing layers or in the chamber itself. The depth distribution of the starting points of Pb-jets (those from interactions in the chamber) enabled an estimate of the interaction length of nuclear active particles in lead to be made. A value of $\lambda_N = (191 \pm 29) gm.cm^{-2}$ was found.

The production rate of nuclear interations was obtained from the observed frequency of Pb-jets after a correction for absorption in the upper chamber and producing layer had been made. The energy spectrum of nuclear active particles was then obtained using as the absolute value

$$I_N(E_\gamma > 3TeV) = (4.3 \pm 0.5) . 10^{-10} cm^{-2} sec^{-1} sterad^{-1}$$

where E_γ was the total energy converted into γ-rays in the interaction. The exponent of the spectrum was $\beta_N = 1.9 \pm 0.3$.

The spectrum is shown in Figure 4.1 and is consistent with the earlier results of Akashi et al (1965).

The energy of the interacting particles was estimated by two methods:

a) The number of shower tracks in a given circle was counted using a microscope and this was compared with the theoretical

value (Nishimura 1965) and the energy determined from this.

b) Opacity measurements were made on the dark spots on the emulsion and again by comparing with the theoretical values the energy was calculated.

The correlation between the two methods was found to be fairly good. The intensities given by Akashi et al and shown in Figure 4.1 are considerably lower than those of Kamata et al. It was pointed out that the latter results were expected to be an upper limit to the spectrum but nevertheless those of Akashi do appear to be very low.

4.3.3 Baradzei et al (1963)

These authors studied the nuclear active particle spectrum at an atmospheric depth of 455 gm.cm^{-2}. The apparatus consisted of a series of ionisation chambers and absorbers the aperture of the arrangement being approximately 1.5 m^2 sterad. The apparatus was flown in an airplane and the flux of unaccompanied hadrons was measured. The energy range covered was 150 to 2000 GeV and the measured spectrum is shown in Figure 4.1.

4.4 Measurements at ~700 gm. cm^{-2}.

4.4.1 Dobrotin et al (1965)

This group have carried out an experiment at the Tien-Shan high altitude station (3340 metres above sea level). It has been used to investigate the strong interactions of cosmic ray nucleons and pions

in the energy range 100-1000 GeV. The apparatus consisted of a cloud chamber in a magnetic field (maximum detactable momentum of 25 GeV/c), an ionisation calorimeter (500 ionisation chambers separated by lead and iron absorbers) and a lithium hydride (LiH) target. Counters were also present which enabled charged and neutral primary particles to be distinguished. (A proposed modification to the apparatus is the construction of an upper cloud chamber which will serve to measure the ionisation produced by a primary particle in xenon with a precision sufficient to distinguish between protons and pions in the energy range 100-1000 GeV. It will also serve to calibrate the ionisation calorimeter).

The energy of the incoming nuclear active particles was measured by the ionisation calorimeter which contained a total of eight nuclear interaction lengths. The centre section of the calorimeter had an area of approximately 10 square metres and the electronic circuits enabled bursts within the range 6 - 12000 relatavistic particles to be measured. The ionisation chambers in adjacent trays were mutually perpendicular so that the arrival direction of the primary particles could be calculated. It was estimated that the root mean square error in determining the primary energy was about 20%.

The vast majority of primary particles interacted in the absorber layers of the calorimeter and for these interactions the following information was obtained:

(i) the cross-section of interactions of nucleons with nuclei of lead and iron in the energy range 10^2 - 10^3 GeV.

(ii) the energy spectra and fluxes of nucleons and pions at an altitude of 3240 metres above sea level.

(iii) the average and individual characteristics of the development of nuclear cascades in iron (Denisov et al (1965)).

The installation has been operated for about 1500 Hrs and for the data analysed an integral spectrum of nuclear active particles of the form $N(>E) = AE^{-\gamma}$ with $\gamma = 1.7 \pm 0.2$ was found for $E > 300$ GeV. The absolute flux was

$$N(>300) = (4.3 \pm 0.5) \quad m^{-2}\ hr^{-1}\ sterad^{-1}.$$

The flux (Figure 4.2) is in agreement with that of Alekseeva et al (1963) but is only about $\frac{1}{2}$ to $\frac{1}{3}$ that given by Pal (1964).

The cross-section measurements indicate that σ_{inel}(iron) = 740 $\pm$ 110 mbn in the range 200-600 GeV and while the precision is much worse there appears to be no significant increase of this value in the range 1200-3000 GeV.

4.4.2 Alekseeva et al (1963)

Nuclear active particles were studied with an ionisation calorimeter at an altitude of 3260 metres above sea level. The calorimeter consisted of twelve layers of ionisation chambers. Nine

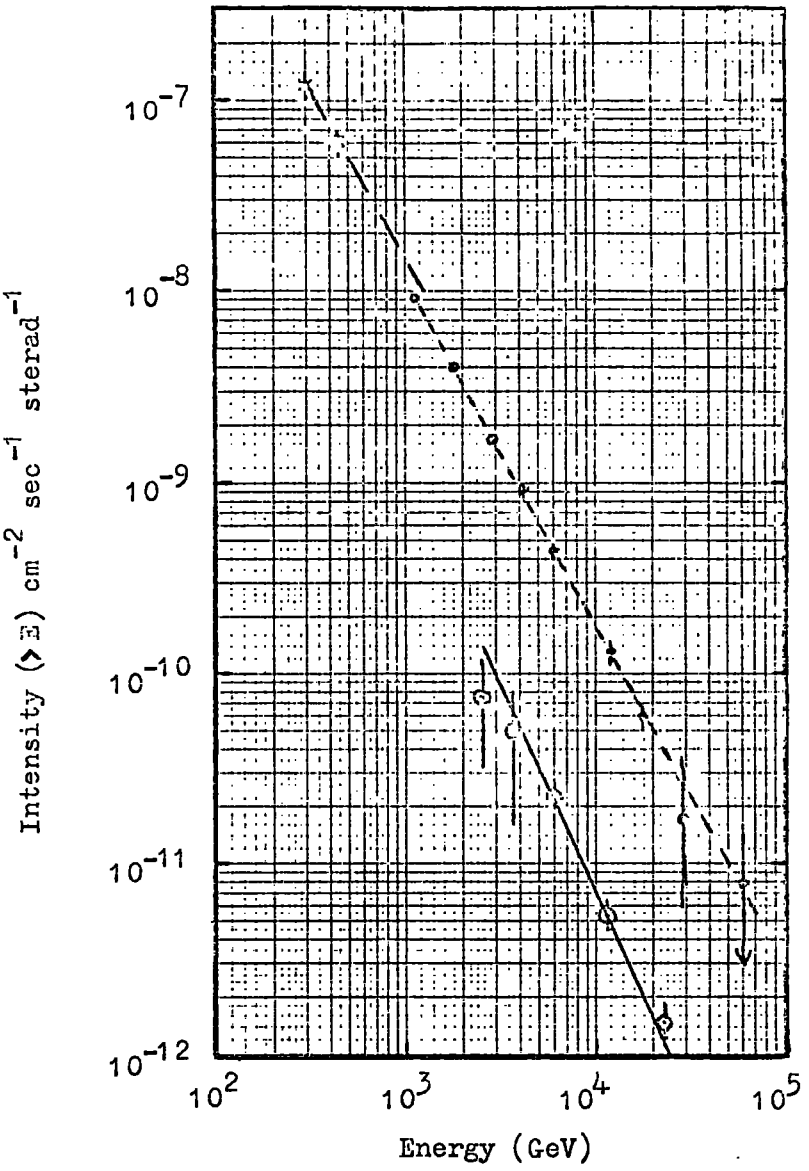

Figure 4.2 Flux of Nuclear Active Particles at $\sim 700 gm.cm^{-2}$.

- Alekseeva et al (1963).
- Dobrotin at al (1965).
- Grigorov et al (1967).
- Akashi et al (1965).

of these layers were situated under uniform layers of iron (total thickness of iron being 670 gm.cm^{-2}). The upper three layers were separated by three layers of lead each having a thickness of 20 gm.cm^{-2}. A cloud chamber was situated above the calorimeter and used to study the angular distribution of the secondary particles produced in the filters above the chamber. Also placed above the calorimeter were counters whose purpose was firstly to measure the charge of the incoming particles and secondly to detect nuclear active particles which were accompanied by air showers. Events were recorded whenever an energy release of $>$ 200 GeV occurred in the calorimeter.

In the range 200 GeV up to approximately 3000 GeV the nuclear active spectrum was found to be of the general form $N(>E) = AE^{-\gamma}$ where,

$$\gamma = 1.92 \pm 0.10 \text{ for accompanied particles}$$

$$\gamma = 2.10 \pm 0.15 \text{ for unaccompanied single particles}$$

The absolute intensity of particles above 450 GeV was

$$N(\geqslant 450 \text{ GeV}) = (6.0 \pm 1.0).\ 10^{-8} \text{ cm}^{-2} \text{ sec}^{-1} \text{ sterad}^{-1}$$

Measurements of the cross-section of nuclear active particle interactions in iron were made, these being estimated from the distribution of interaction points in the calorimeter. It was found that

$$\lambda_{int} \text{ (iron)} = (138\ ^{+11}_{-9}) \text{ gm.cm}^{-2}$$

Cross-section measurements for interactions in the carbon and lead filters were also made with the following results

$$\lambda_{int}(C) = (90^{+20}_{-15}) \text{ gm.cm}^{-2}$$

$$\lambda_{int}(Pb) = (176^{+64}_{-32}) \text{ gm.cm}^{-2}$$

c.f. Dobrotin et al (1965): $\lambda_{int}(Fe) = (127 \pm 19) \text{ gm.cm}^{-2}$

Akashi et al (1967): $\lambda_{int}(Pb) = (191 \pm 29) \text{ gm.cm}^{-2}$

4.4.3 Grigorov et al (1967)

A measurement was made of the spectrum of nuclear active particles at an altitude of 3200 metres above sea level using an ionisation calorimeter. The energy range covered was 10^{12} eV to 10^{14} eV and two installations each of area 10 sq. metres were used in the experiment. One consisted of six trays of ionisation chambers and combined filters of lead and graphite while the other had twelve trays of ionisation chambers and filters of lead, graphite and iron. The apparatus was operated for a total of 1108 hours and the integral spectrum from each of the two sections calculated. These two spectra were then averaged to give the spectrum of bursts which had an exponent of 1.86 ± 0.04. The cascade curves of Ivanenko and Samosudov were then used to convert this burst spectrum into the energy spectrum of nuclear active particles at 3200 metres. This spectrum is shown in Figure 4.2 and is seen to be in good agreement with the fluxes obtained by Alekseeva and Dobrotin.

4.4.4 Erlykin et al (1967)

This group have been using a calorimeter telescope primarily to check the hypothesis of the existence of the passive baryon state but also to look at the energy spectrum of nuclear active particles. The apparatus was situated at the Tien-Shan mountain station an altitude of 3200 metres above sea level. It was estimated that individual particle energies could be determined to an accuracy of $\pm$ 30% and the preliminary results indicate a spectrum with exponent 1.68 ± 0.15 in the energy range 5.10^{11} eV to 10^{13} eV.

4.4.5 Akashi et al (1965)

In section 4.3.2 the results of an experiment at Mount Chacaltaya were described. A similar experiment has been performed at Mount Norikura, an altitude of 2800 metres above sea level. The nuclear active spectrum measured here is shown in Figure 4.2 and as with the higher altitude results the intensities are considerably lower than those of other experiments.

4.5 Measurements at Sea Level

4.5.1 Cowan and Moe (1967)

A calorimeter experiment, 250 metres above sea level, was performed to look at single nuclear active particles above an energy of 140 GeV. The apparatus consisted of 12 flat cloud chambers and 8 flat ionisation chambers which could be interleaved with various combinations

of absorbers. The top cloud chamber located the track of the single incoming charged particle. Below this was a carbon target of thickness 111 $gm.cm^{-2}$ and the showers produced in it were looked at in the following ten cloud chambers and then in the ionisation calorimeter. A final cloud chamber below the calorimeter served to identify particles which had penetrated the whole stack. The aperture of the instrument was 0.22 m^2 sterad. The cloud chamber information and the pulse heights from the ionisation chambers were all recorded photographically.

Results show that the flux of nuclear active particles with energy greater than 140 GeV is

$$(1.3 \pm 0.1)\ 10^{-4}\ m^{-2}\ sec^{-1}\ sterad^{-1}.$$

This value is lower than the estimated flux probably because of the requirement that there must be no accompanying particles within the 0.22 m^2 sterad.

A separate experiment has been performed to estimate the relative proportions of protons and pions. A total of 138 charged (protons and pions) and 47 neutrals (neutrons) have been recorded. Baradzei (1963) gives a π: N(n+p) ratio of 0.29. Combining that with the result of the experiment described here gives 70% protons and 30% pions for the relative proportions at sea-level with energy $>$ 140 GeV. The ratio of protons to neutrons under these conditions, however, would be about 2:1.

4.5.2 Brooke and Wolfendale (1964a)

A magnetic spectrometer has been used to measure the sea level momentum spectrum of cosmic ray protons in the range 0.6 to 150 GeV/c. The protons were deflected in a region of high magnetic field produced by an electromagnet and their positions measured at four levels - two above and two below the magnet. The protons can be identified in two ways: (a) by their absorption, either through ionisation loss or catastrophic interaction, in local obsorbers, or (b) through their production of evaporation neutrons using a neutron monitor. Both techniques were used in the low energy region but only method (b) was used at higher energies as the absorption technique becomes unreliable since the probability of a secondary emerging from the absorber becomes higher.

The spectrometer was run for a total of 2420 hours and the measured differential momentum spectrum of protons is shown in Figure 4.3. The only other sea level measurement of the proton spectrum to compare with this is that given by Mylroi and Wilson (1951). This agrees with the measurement of Brooke and Wolfendale up to about 2 GeV/c above which the intensities of the former become lower.

An estimate of the proton to muon ratio has also been made. The results showed that this ratio fell as the momentum increased, being about 6% at 0.7 GeV/c and 0.4% over the momentum range 50 - 150 GeV/c.

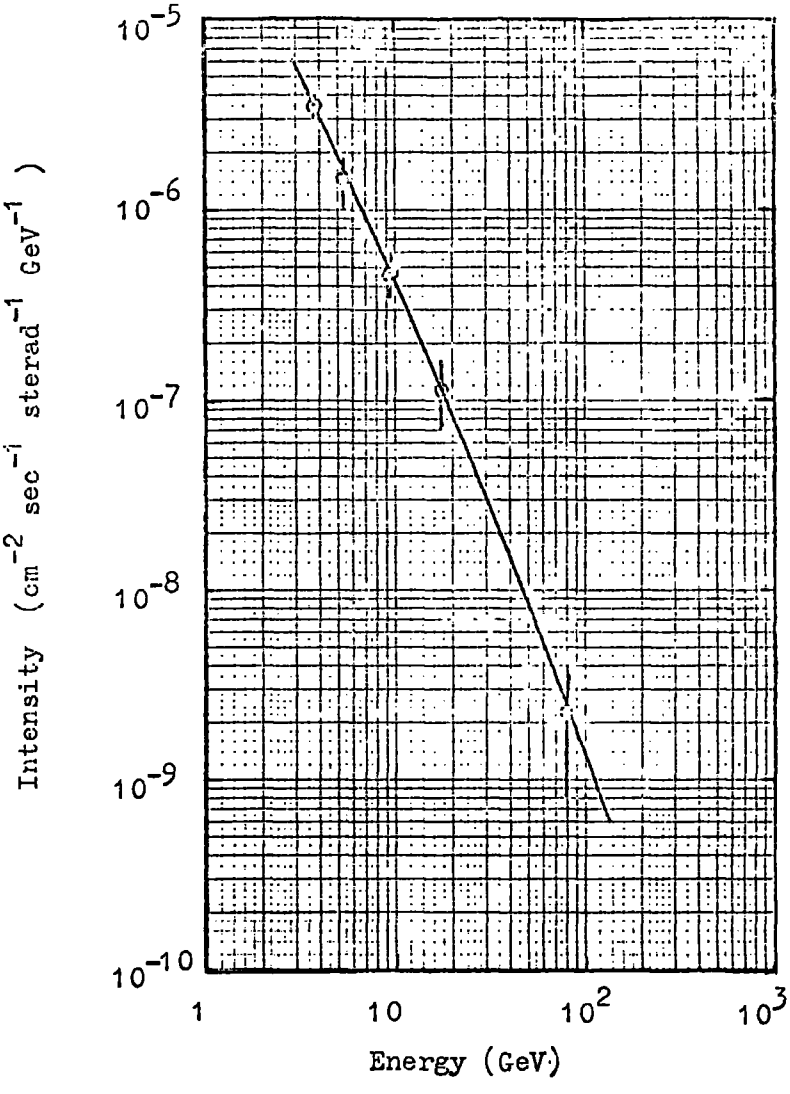

Figure 4.3 Differential Sea Level Proton Spectrum according to Brooke et al (1964a).

4.5.3 Kellermann and Silk (1965)

These authors operated a small nuclear calorimeter consisting of five trays of proportional counters, each tray having an area $0.73m^2$, in a matrix of lead and steel absorber. The apparatus was situated at sea level and nuclear active particles in the energy range 5.10^{10} - 5.10^{12} eV were selected. A total of 2437 events were recorded at the rate of (8.1 ± 0.1) $m.^{-2}$ $hr.^{-1}$ and the exponent of this burst spectrum was found to be $-(2.15 \pm 0.10)$.

After separating out the muon induced bursts the spectrum of bursts produced by nuclear active particles was found to have an exponent of -1.8 ± 0.1 up to a burst size of 1600 particles (about 10^{12} eV). The rate of events as well as the slope of the spectrum are compatible with the proton spectrum given by Brooke and Wolfendale (1964) and that of nucleons of comparable energies entering emulsion stacks, Fowler and Perkins (1964). Results also indicate that the ratio of muon to nuclear active particle initiated bursts at a burst size of around 100 particles is of the order of 4:5 this being in agreement with Tanaka (1961).

Finally investigations also showed that there was no obvious relation between the burst size produced by a nuclear active particle and the size of an accompanying air shower.

4.6 Conclusions

A summary of the various experimental results on the nuclear

active particle flux at different atmospheric depths is given in Table 4.1. The measurements have also been summarised in Figure 4.4. Each intensity has been multiplied by a factor $e^{X/100}$ and it can be compared with the primary nucleon spectrum. It will be seen that the different experiments yield an exponent between 1.6 and 2.0 for the integral spectrum and there seems to be reasonable agreement with regard to absolute intensities apart from one measurement, that of Akashi et al (1967).

A great many of these experiments determine simply the flux of hadrons making no distinction between the individual components. It would appear that further progress in studying the nucleon propagation in the atmosphere can most effectively be made by performing identical experiments at different atmospheric depths, these experiments being so designed that the spectrum of one of the nuclear active components is measured, as it is practically very difficult to measure more than one individually at the same time.

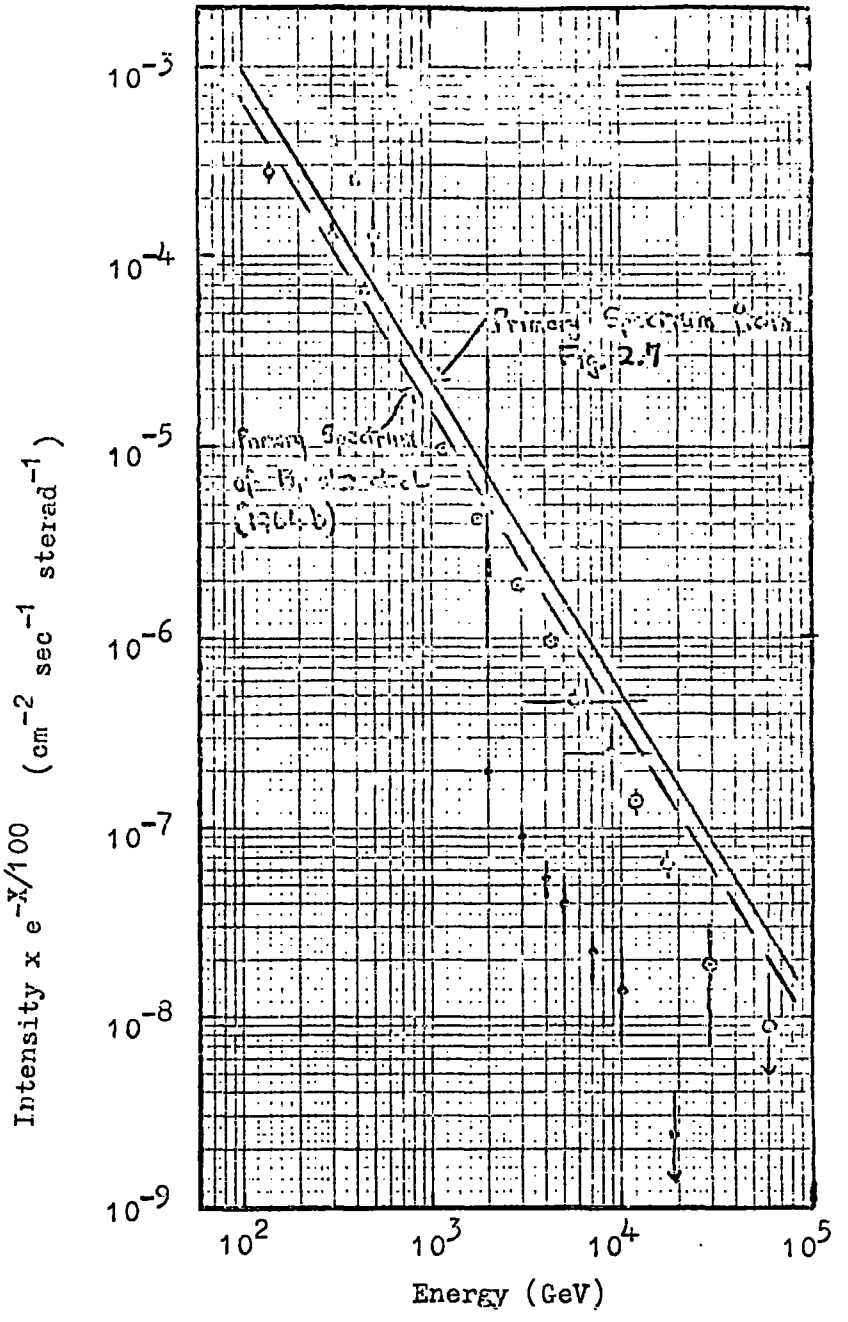

Figure 4.4 Comparison of the various Nuclear Active Particle Spectra. Each intensity has been multiplied by a factor $e^{-x/100}$.

- ▣ Baradzei et al (1963) - 455 gm.cm^{-2}.
- • Akashi et al (1967) - 550 gm.cm^{-2}.
- ⊙ Grigorov et al (1967) - 700 gm.cm^{-2}.
- ▲ Dobrotin et al (1965) - 700 gm.cm^{-2}.
- ▣ Alekseeva et al (1963)- 700gm.cm^{-2}.
- ○ Cowan and Moe (1967) - 1000 gm.cm^{-2}.
- ▲ Kamata et al (1967) - 550 gm.cm^{-2}.

TABLE 4.1 SUMMARY OF EXPERIMENTS

Experiment	Exponent of Spectrum	Depth	Further Details
Kamata et al	≤ 2.0 for surviving primary protons.	$530 g.cm^{-2}$	σ(N-air) 270mb, i.e. σ(N-N)$>$27mb at 10^{13}eV
Akashi et al	1.9 ± 0.3	$530 g.cm^{-2}$	λ_i(Nucl. Int. in Pb) $= 191 \pm 29$ $g.cm^{-2}$
Baradzei et al	~ 2.0	$455 g.cm^{-2}$	
Grigorov et al	1.86 ± 0.04	$700 g.cm^{-2}$	
Dobrotin et al	1.7 ± 0.2	$700 g.cm^{-2}$	σ (N-Fe) 740 ± 110mb (for 200-3000 GeV)
Alekseeva et al	1.92 ± 0.10 (acc.) 2.10 ± 0.15 (unacc.)	$700 g.cm^{-2}$	λ_i(N-Fe)$=(138^{+11}_{-9})$ $g.cm^{-2}$
Erlykin et al	1.68 ± 0.15	$700 g.cm^{-2}$	
Cowan and Moe		$1000 g.cm^{-2}$	$I(>140GeV) = (1.3.10^{-8})$ $(cm^{-2}\ sec^{-1}\ st^{-1})$.
Brooke and Wolfendale	1.6	$1000 g.cm^{-2}$	Sea Level Proton Spectrum
Kellermann and Silk.	1.8 ± 0.1 (Burst Spectrum)	$1000 g.cm^{-2}$	$\frac{\mu}{N.A.}$ bursts $= \frac{4}{5}$

CHAPTER 5

THEORY OF BURST PRODUCTION IN A THICK IRON ABSORBER

5.1 Introduction

Experiments to measure the spectra and study the interactions of high energy nuclear active particles in the atmosphere usually employ some type of calorimeter experiment. In the main these consist of a thick high density target material in which the nuclear active particle is required to interact and below which are a series of thin detectors and absorbers enabling the development of the cascade produced in the nuclear interaction to be studied. The energy of the interacting particle is normally estimated from the ionisation produced by the particles in the cascade. It is necessary, therefore, in the analysis of the results of these experiments to adopt some model for the interaction of the high energy nuclear active particle in the absorber as well as for the cascade subsequently produced so that a reliable estimate of the particle energy can be made.

In this particular experiment in which a study has been made of high energy neutrons in the sea level cosmic radiation the target was 1.35 nuclear interaction lengths of iron and the burst was detected and measured by a liquid paraffin scintillation counter. The generally accepted picture of a high energy nucleon interacting in such a target is as follows. On entering the absorber the probability that the nucleon undergoes an interaction follows the exponential

law $e^{-X/\lambda}$ where X is the thickness of the target and λ the interaction length. After a collision the nucleon retains a certain fraction of its initial energy, the majority of the energy lost going into the production of pions. It is assumed that the number of charged pions is twice the number of neutrals. The neutral pions immediately decay into two gamma rays which can then initiate an electron-photon cascade either by materialising into an electron-position pair or by undergoing Compton scattering. The charged pions interact deeper in the absorbing medium producing more pions the neutral ones again decaying into two gamma rays. The electrons which are produced in the pair production and Compton scattering of these photons can then produce more photons by radiation loss (bremsstrahlung), assuming the critical energy of the medium (ϵ_o) is much less than the electron energy, and these photons in turn produce further electrons. Thus an electron-photon shower is built up in the medium. In a substance such as iron where the radiation length and critical energy are relatively small this process occurs quite quickly. After a certain distance the average energy of the electrons will fall to a value below that of the critical energy and the cascade will die out, all the energy being lost to excitation and ionisation in the target

The theoretical treatment of electron-photon showers in various media has been studied extensively by many workers. Broadly speaking there have been two lines of approach:

a) The Analytical Method. The development of the shower at a

given depth is represented by a series of diffusion equations. These are solved by introducing simplifying assumptions.

b) The Monte-Carlo Method. Different primary particles and their secondaries are followed through the absorbing medium, the fate of each being determined by a "wheel of chance".

In this chapter a brief discussion of the various solutions to the problem of the electron-photon shower development will be given. The model used for the interaction of nucleons in the iron target will be discussed and a relationship established between the energy of the interacting nucleon and the burst size detected by the scintillation counter. This result will then be compared with the cascade curves for nuclear interactions in iron given by Pinkau and Thompson (1966).

5.2 The Electron-Photon Shower and its Treatment

5.2.1 General

The problem of deriving the number of electrons and photons at a given depth in a substance produced by a primary electron or photon of energy E_o is mathematically very difficult. Many problems concerned with electron-photon showers require only a knowledge of their average behaviour and these average quantities are much easier to derive than say the probability for the number of particles to

have a predetermined value. Most calculations on shower theory just refer to the average behaviour, the probability of finding specific numbers being treated as a fluctuation problem; that is the probability of a given deviation from this average behaviour is estimated. However, the fluctuation problem is also extremely difficult and again several simplifying assumptions have to be made.

5.2.2 The Analytical Method

The problem of dealing mathematically with electron-photon showers has been discussed in detail by Rossi (1952). The various processes such as pair production and Compton scattering by photons and bremsstrahlung and ionisation losses by electrons, which occur during the development of the cascade, are all dealt with. In the analytical method the procedure has been to derive a set of equations which describe the variation with thickness in the numbers of electrons and photons of each energy interval. At any thickness t the number of electrons and photons with energies between E and E+dE can be represented respectively by $\pi(E,t)\,dE$ and $\gamma(E,t)\,dE$. These numbers vary as the radiation traverses an additional thickness dt because of the pair production etc. mentioned above and this variation is described by the following set of diffusion equations.

$$\frac{\partial \pi(E,t)}{\partial t} = + \int_{E}^{\infty} \gamma(E',t)\, \phi_p(E,E')dE' + \int_{E}^{\infty} \pi(E',t)\phi_E(E',E'-E)dE'$$

$$- \int_{0}^{E} \pi(E,t)\phi_E(E,E')dE' - \epsilon(E) \frac{\partial \pi(E,t)}{\partial E}$$

$$\frac{\partial \gamma(E,t)}{\partial t} = \int_{E}^{\infty} \pi(E',t)\phi_E(E',E)dE' - \int_{0}^{E} \gamma(E,t)\phi_p(E,E')dE'$$

where,

$\epsilon(E)$ represents the average ionisation loss per radiation length.

$\phi_E(E,E')$ is the differential probability per radiation length for an electron of energy E to produce a photon of energy E'.

$\phi_p(E,E')$ is the differential probability per radiation length for a photon energy E to produce an electron energy E' either by pair production or Compton scattering.

5.2.3 Solutions by Approximation A and Approximation B

It has been stated earlier that in order to solve these diffusion equations certain simplifying assumptions have to be made. Two methods which introduce two different sets of these assumptions are known as

Approximation A and Approximation B resepctively.

In Approximation A only those energies large compared with the critical energy are considered so the theory of showers can be developed by dealing only with radiation phenomena and pair production. Furthermore, it has been shown by Rossi (1952) that if the energies under consideration are restricted to those large compared with the factor $137m_e c^2 Z^{\frac{1}{3}}$, radiation phenomena and pair production can be described by the asymptotic formulae for complete screening. Thus the assumptions under Approximation A are to neglect the Compton effect and collision losses and to describe the probabilities for radiation processes and pair production by their asymptotic formulae. It is interesting to note that under Approximation A shower theory yields identical results for all materials provided thicknesses are measured in radiation lengths.

When the energies involved become comparable with the critical energy the Compton effect can still be disregarded but collision processes must be taken into account. These, however, do not contribute appreciably to the production of secondary electrons and the effect need only be considered in terms of its influence on the energy loss of electrons. Under Approximation B, therefore, it is assumed that the Compton effect can be neglected, collision loss is described as a constant energy dissipation and the asymptotic formulae for radiation loss and pair production are used. Approximation B gives identical results for all elements provided the thicknesses

are measured in units of radiation length and energies in terms of the critical energy. It should be noted that the basic assumptions of Approximation B make it more suited to light as opposed to heavy elements.

The solutions of the diffusion equations under Approximation A and Approximation B are described in detail by Rossi (1952) and examples of the cascade curves which result are shown in Figure 5.1.

A comprehensive survey of the different attempts which have been made to solve the problem of electron-photon showers has been given by Belenkii et al (1959). The various solutions to the diffusion equations are discussed together with the assumptions under which they are valid.

5.2.4 Method of Moments : Cascades in Iron

The methods of Approximation A and Approximation B which utilise what are known as functional transformations to solve the diffusion equations give a fairly complete solution to the problem of describing one-dimensional cascades in light elements. The method of functional transforms, however, breaks down in light elements when the energy of the particle which initiates the cascade becomes comparable with the critical energy of the medium in which the shower develops. This method is also invalid in heavy elements for the following two reasons:

a) the scattering of the shower particles in heavy elements is large.

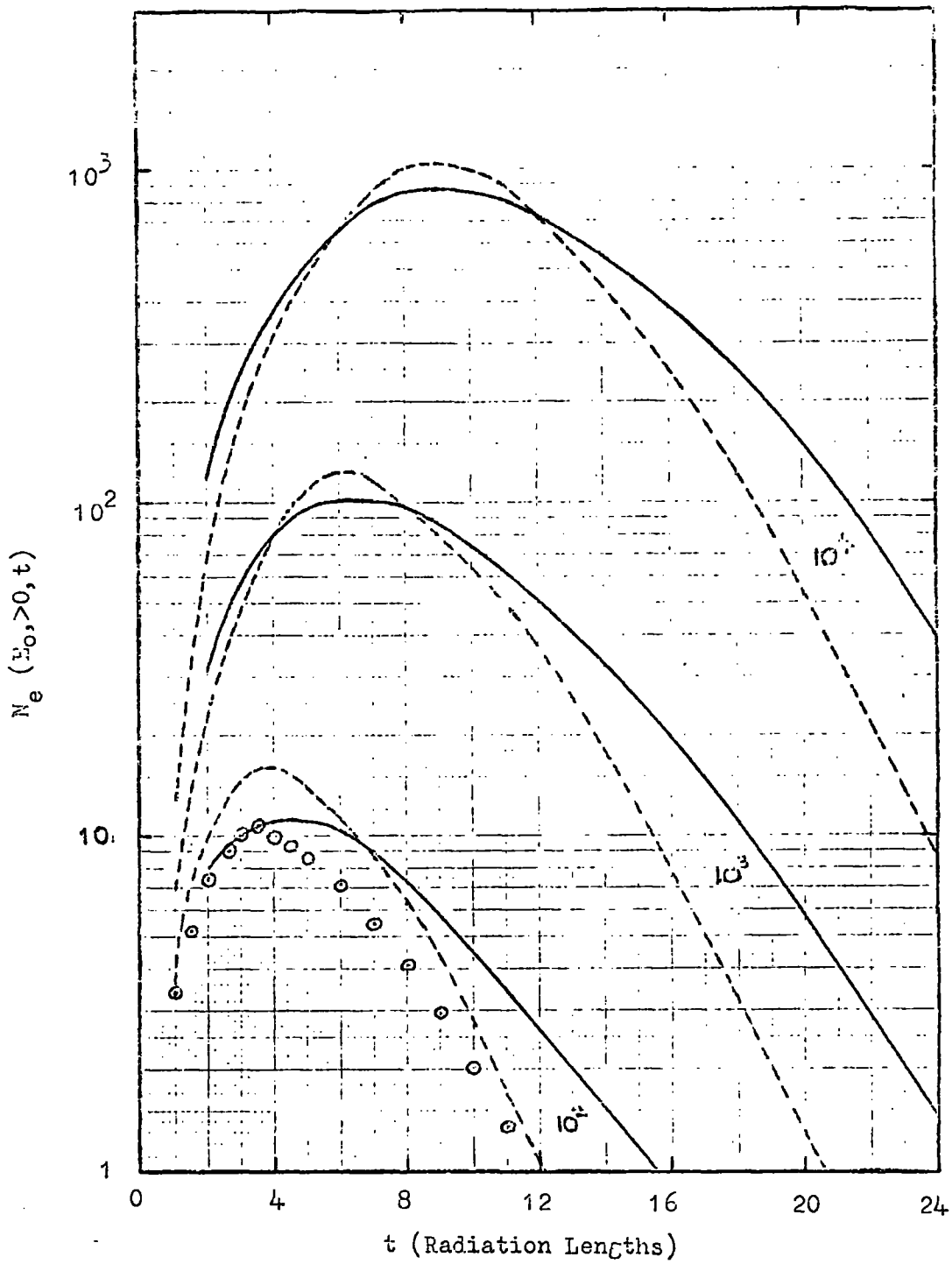

Figure 5.1 Shower development curves of Approximation B (broken lines) and Ivanenko et al (full lines) for cascades initiated in iron by electrons of energy $E_o/\epsilon_o = 10^2, 10^3, 10^4$, where ϵ_o = 21 MeV, the critical energy in iron. The points ⊙⊙⊙⊙ are from the Monte Carlo calculations of Crawford et al (1965) for an energy of $E_o/\epsilon_o = 95$.

b) the total photon absorption coefficient depends strongly on the energy.

An alternative method in the solution of this problem and one which has been applied to heavy absorbers (Belenkii et al (1959)) is known as the method of moments. This has been described by Ivanenko (1957). The method makes use of the fact that the distribution fuction of shower particles can be described by its moments which are calculated sucessively from an "equilibrium" spectrum of electrons and photons.

In the neutron spectrum experiment the shower is developed in an iron absorber and bursts are induced by photons with average energies in the range 1 GeV to 30 GeV. Thus in the calculation of expected burst sizes the electron-photon shower curves employed must be applicable to iron and cover the relevant energy range. Ivanenko and Samosudov (1959) have produced a series of shower curves which apply to copper but which can also be used for iron since the Z for copper is only about 10% different from that of iron. The curves have been calculated for primary electron and photon energies in the range $10^7 \leqslant E \leqslant 10^{12}$ eV which includes the range required for this experiment. The method of moments was used to calculate the total number of electrons and photons and account was taken of the scattering of charged particles and also of the energy dependence of the total photon absorption coefficient. As these curves are directly applicable to an iron absorber it has been decided to adopt them in

calculating the burst sizes expected in the scintiallation counter. The curves are shown in Figure 5.1 and a comparison with the results of Approximation B can be made. Shower development curves are plotted for cascades initiated in iron by primary electrons of energies E_o given by $E_o/\epsilon_o = 10^2$, 10^3 and 10^4 where ϵ_o (the critical energy in iron) = 21 MeV. These curves give the total number of electrons at any depth t measured in radiation lengths. The results of Ivanenko et al can be seen to differ from those of Approximation B in the region after shower maximum. This arises because of the approximations involving the use of asymptotic values introduced in the latter method. In Figure 5.2 and Figure 5.3 are displayed the cascade curves for electron and photon initiated showers. Loci of constant age parameter s are also shown.

5.2.5 Comparison of Theory with Experiment

Coats (1967) has surveyed the experimental information on electron-photon showers. An accelerator experiment by Backenstoss et al (1963) looked at average showers in iron up to energies of 10 GeV. Good agreement was found between the measured number of electrons and the theory of Ivanenko for showers of energy $\leqslant 4$ GeV but at 10 GeV theory predicted about 20% more electrons at shower maximum than were observed. There are also two calorimeter type experiments one by Takbaev et al (1965) and one by Murzin et al (1963) which looked at electromagnetic cascades produced in iron absorbers.

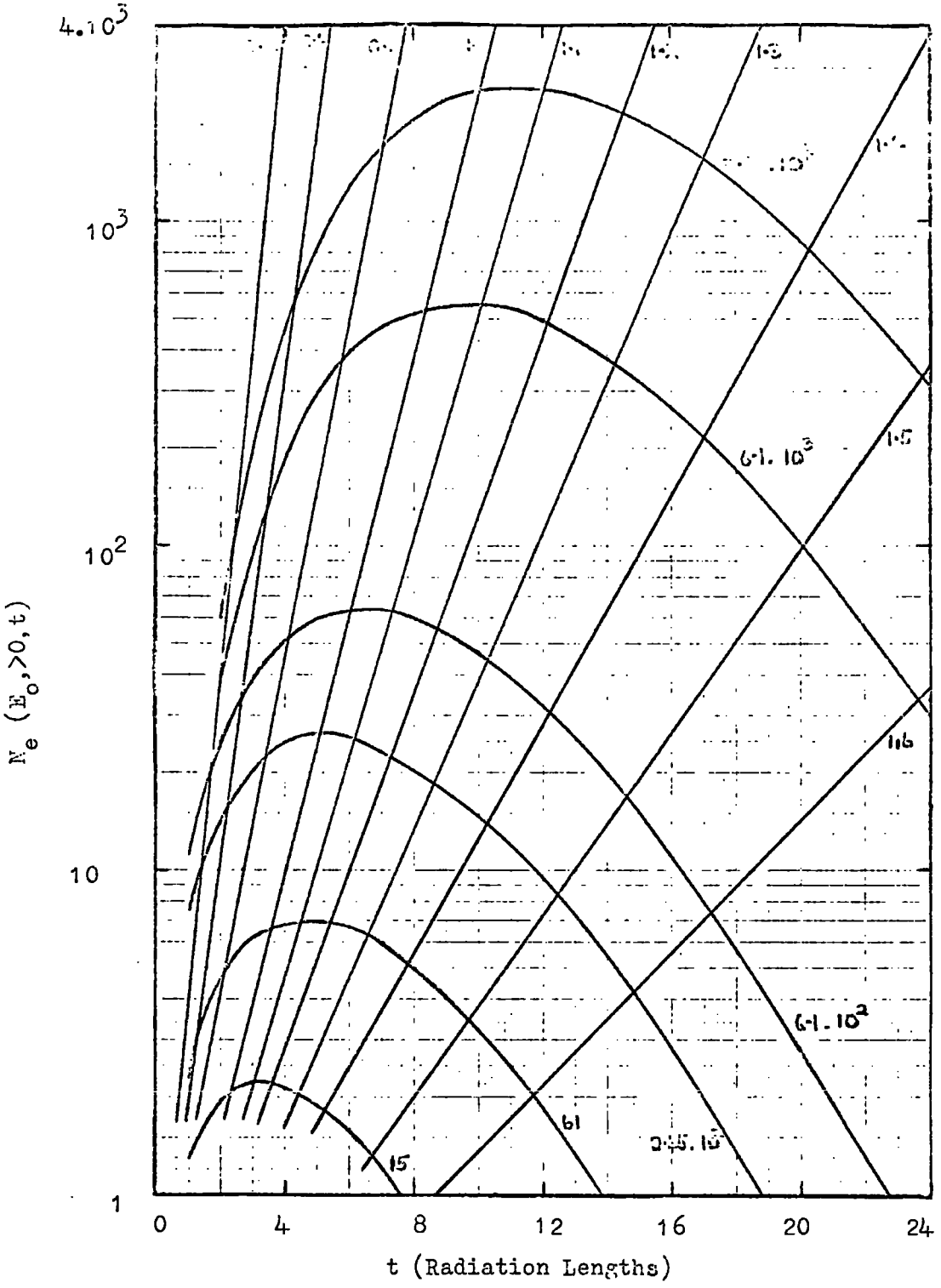

Figure 5.2 Shower development curves giving the total number of electrons as a function of depth for cascades initiated in iron by electrons with energy E_o/ϵ_o=15, 61, $2.45.10^2$, $6.1.10^2$, $6.1.10^3$, and $3.23.10^4$., according to Ivanenko et al (1958). The straight lines are loci of constant age parameter s.

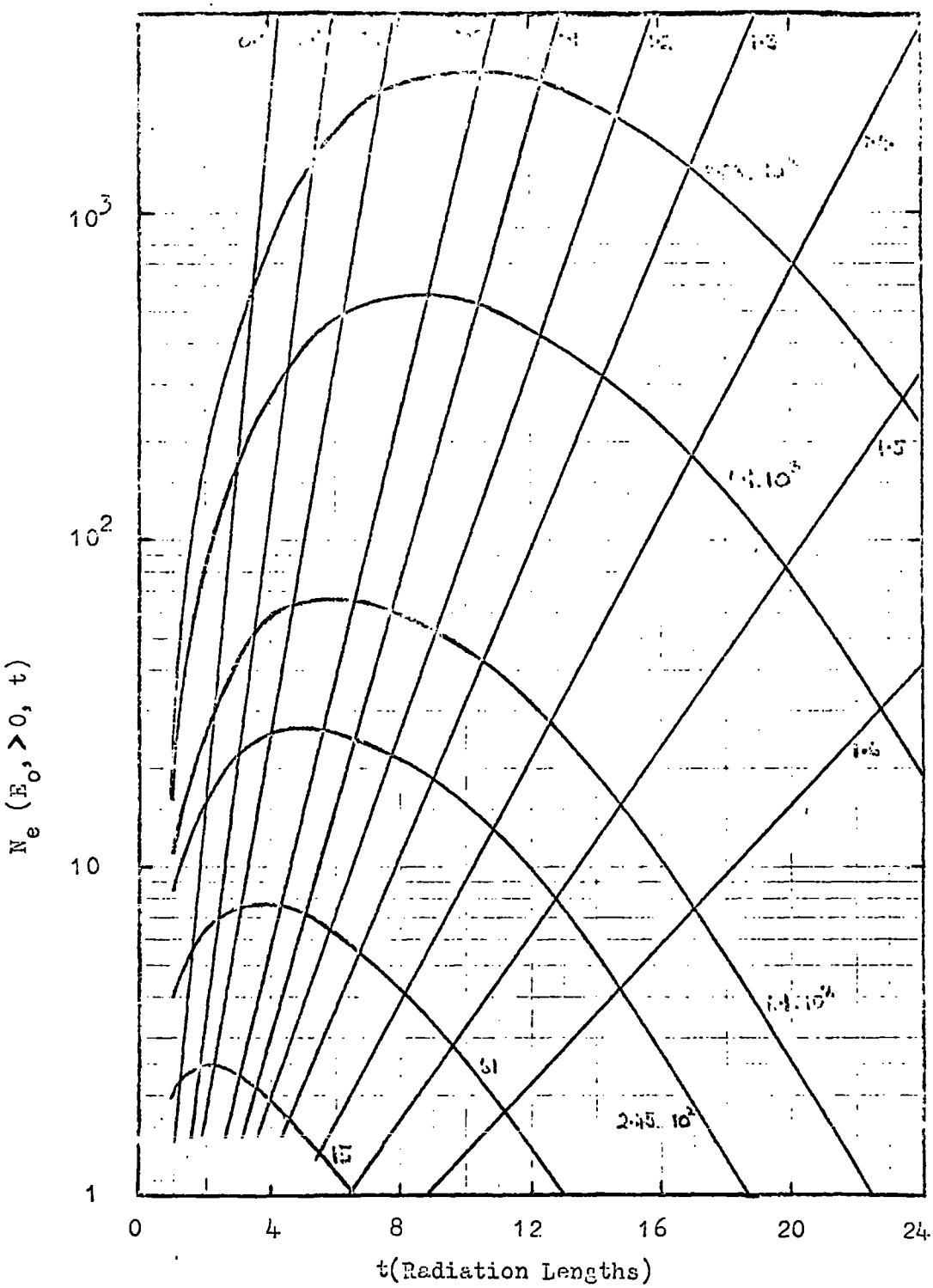

Figure 5.3 Shower development curves giving the total number of electrons as a function of depth for cascades initiated in iron by photons with energy E_o/ε_o=15, 61, $2.45.10^2$, $6.1.10^2$, $6.1.10^3$, and $3.23.10^4$., according to Ivanenko et al (1958). The straight lines are loci of constant age parameter s.

The events in both experiments were normalised to an energy of 100 GeV and the curves and experimental points are shown in Figure 5.4. It can be seen that the experimental measurements agree quite well with the theoretical curve in both cases although it should be noted that the absolute numbers of electrons measured by the two experiments are different despite both being normalised to 100 GeV.

5.2.6 Monte Carlo Calculations

Although several Monte-Carlo calculations have been performed on the development of electron-photon showers there is only one set that applied to an iron absorber and this is restricted in its energy range. The calculations were performed by Crawford et al (1965) and were for a three-dimensional cascade in copper. The limited energy range of these tables means that they cannot usefully be applied to the present problem but they can be used to make a comparison with the curves of Ivanenko et al in the region of overlapping energies. In doing this it should be remembered that Crawford et al give the flux of electrons with energy > 10 MeV while Ivanenko gives the flux of all electrons. The curve for an energy of $E_o/\epsilon_o = 95$ is shown in Figure 5.1 for comparison with Ivanenko et al and Approximation B.

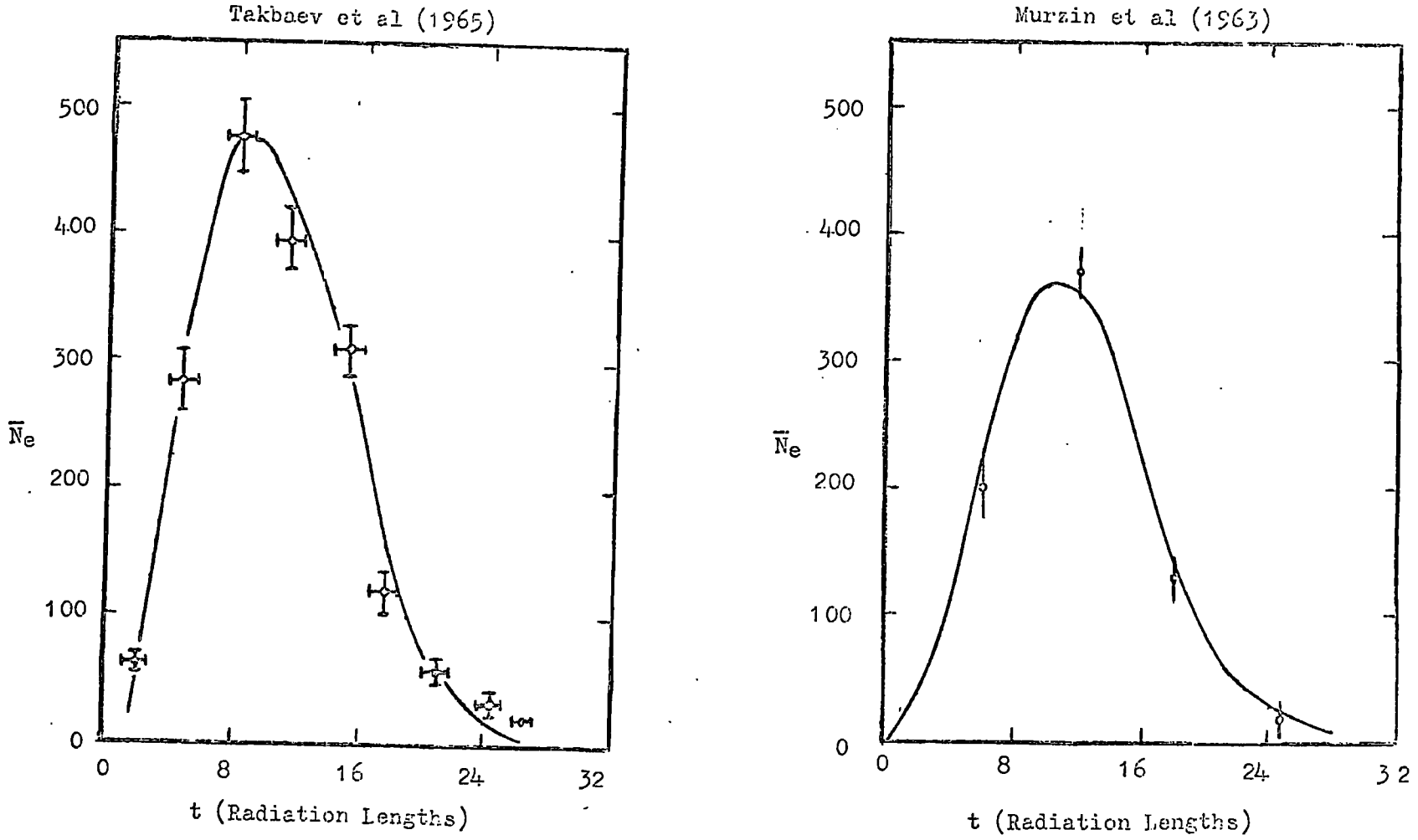

Figure 5.4 Comparison of theoretical curves of Ivanenko et al (1958) with experimental results.

5.3 Burst Size Measured in the Scintillator

5.3.1 General

The purpose of this experiment has been to make an estimate of the high energy sea level neutron spectrum by measuring the spectrum of bursts produced by neutrons interacting in an iron target. The bursts have been detected and measured in a liquid paraffin scintillation counter the size of a burst being measured in terms of an equivalent number of particles where one equivalent particle is defined as the average energy lost by a single relatavistic particle traversing the centre of the scintillator. A scintillation counter essentially measures the track length of an ionising particle in the phosphor and in order to completely traverse the counter such a particle requires a certain minimum energy. The minimum energy for the scintillators in this experiment was 28 MeV.

The electrons in a shower emerging from the iron target will have a spectrum of energies, those with greater than 28 MeV will completely penetrate the counter and each be recorded as one equivalent particle while those with less than 28 MeV will have varying track lengths in the phosphor and each will give a contribution which is some fraction of an equivalent particle. The curves given earlier of the total number of electrons as a function of depth in a given element cannot therefore be applied directly to the measurement of burst size in equivalent particles. They have to be modified so that they represent the burst size measured by the scintillation

counter as a function of depth and in order to do this it is necessary to know the energy spectrum of electrons in a cascade shower. Another factor to be taken into account is the contribution photons make to the burst size. A cascade consists of both electrons and photons and the photons can interact in the phosphor to produce electrons by the processes of pair production and Compton Scattering. These electrons will then contribute to the measured burst size.

5.3.2 Energy Spectrum of Electrons in a Burst

Various attempts to formulate expressions to represent the energy spectrum of electrons in a shower have been made. These have been reviewed by Coats (1967) where a comparison has been made with some experimental measurements on the problem. The best expression appears to be one of the form $N(>E) \propto (E + \epsilon_0)^{-\gamma}$ where γ can be varied. In Figure 5.5 are shown the experimental points of Nassar et al (1946) together with various theoretical predictions. These give the energy distribution of electrons at shower maximum in a 2 GeV cascade initiated by a primary electron. The experimental points were obtained using a counter controlled cloud chamber operated in a magnetic field and the showers measured were produced in lead by a single electron. The points have been normalised to the Ivanenko curve at an electron energy E given by $E/\epsilon_0 = 0.45$ and have been corrected so as to apply to an iron absorber.

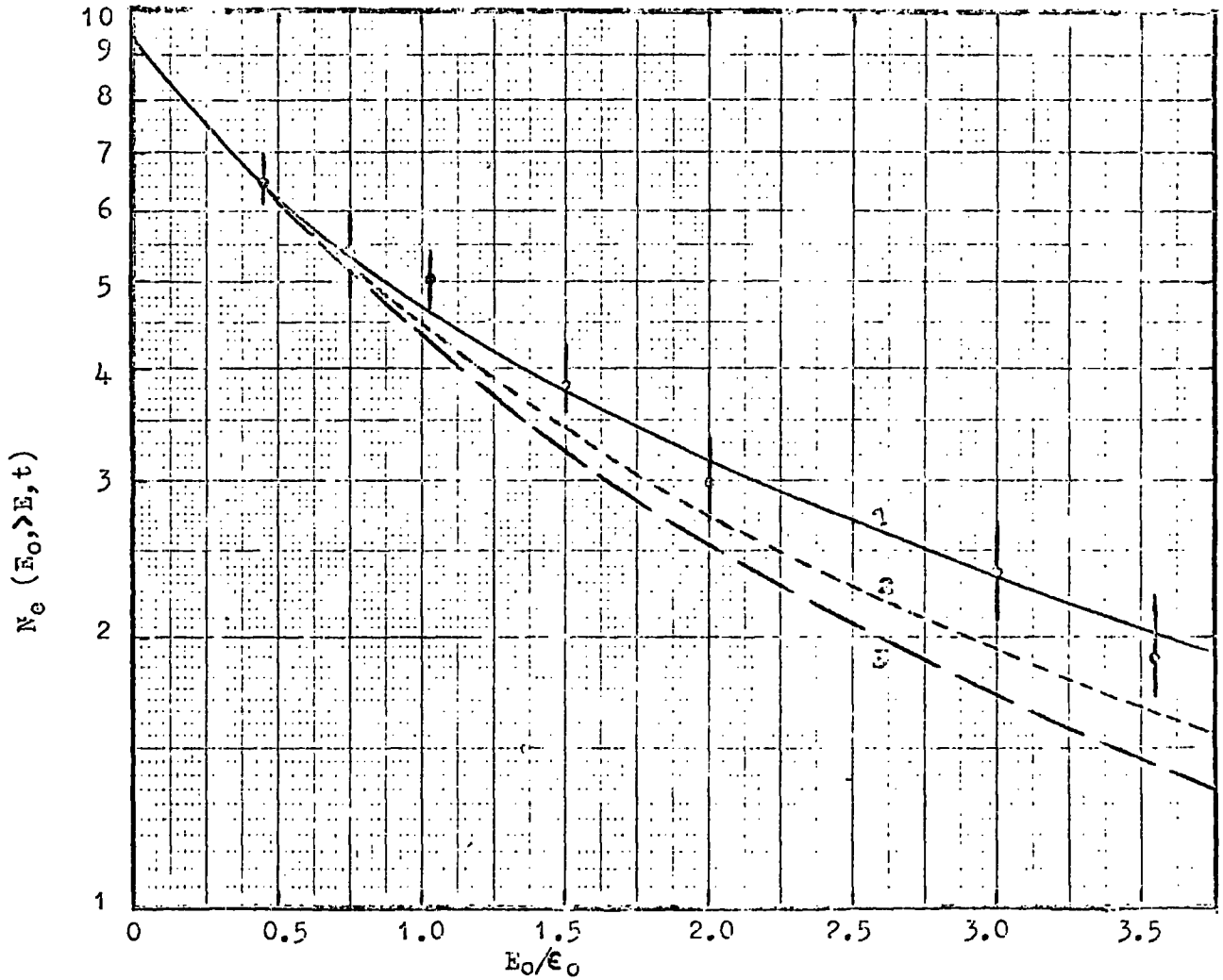

Figure 5.5 Energy distribution of electrons at shower maximum in a 2 GeV cascade initiated in iron by a primary electron.

1. Prediction of Ivanenko using $N(>E) = N(0)/(1+E/\epsilon_o)^s$
2. Richards et al (1948). 3. Crawford et al (1965).
4. Nassar et al (1946).

The expression used to caluclate the energy spectrum from the Ivanenko curves was the following

$$N(>E) = N(>0)\ (1 + \frac{E}{\epsilon_o})^{-s}$$

This appears to give good agreement with the experimental data and so has been adopted for the purposes of the present work.

5.3.3 Photon Contribution to a Burst

Following Coats (1967) the photon contribution to the burst size has been taken as 24%. In calculating this value the curves giving the number of photons as a function of depth were those interpolated from Approximation A described earlier. These were used in conjuction with the probabilities for pair production and Compton scattering given by Rossi (1952) to evaluate the total track length of electrons produced in the phosphor. The energy spectrum of photons was assumed to be the same as that of electrons.

5.3.4 Conclusions

As the theorectical cascade curves of Ivanenko et al appear to be in agreement with the available experimental data these have been adopted for use in the present calculation. The energy spectrum of electrons in a shower are best described by

$$N(>E) = N(>0)\ (1 + \frac{E}{\epsilon_o})^{-s}$$

where ϵ_0 is the critical energy of the medium and s the age parameter.

By integrating this spectrum of electrons over the thickness of the phosphor it can be shown that the burst size measured by the scintillator as an equivalent number of particles is represented by the number of electrons in a shower with energy > 15 MeV. The curves relating burst size measured in equivalent particles as a function of depth in radiation lengths are shown in Figure 5.6 and these include the 24% contribution from photon interactions in the phosphor. These curves have been used in the evaluation of burst sizes produced by nucleons interacting in the iron absorber.

5.4 Nucleon Interactions in Iron

5.4.1 General

Any experiment performed to measure the energy spectrum of neutrons relies on a knowledge of their interactions in both their detection and energy measurement. In this particular case this is achieved by studying the products of neutron interactions in an iron absorber. The energy of the interacting neutrons has to be estimated from the burst size that is measured by the scintillation counter and in order to do this a model for their interactions with iron nuclei has to be adopted. The various features of this model such as inelasticity and multiplicity values will now be described.

In the calculations it has been assumed that after the nucleon-iron nucleus interaction the nucleon emerges with half its initial

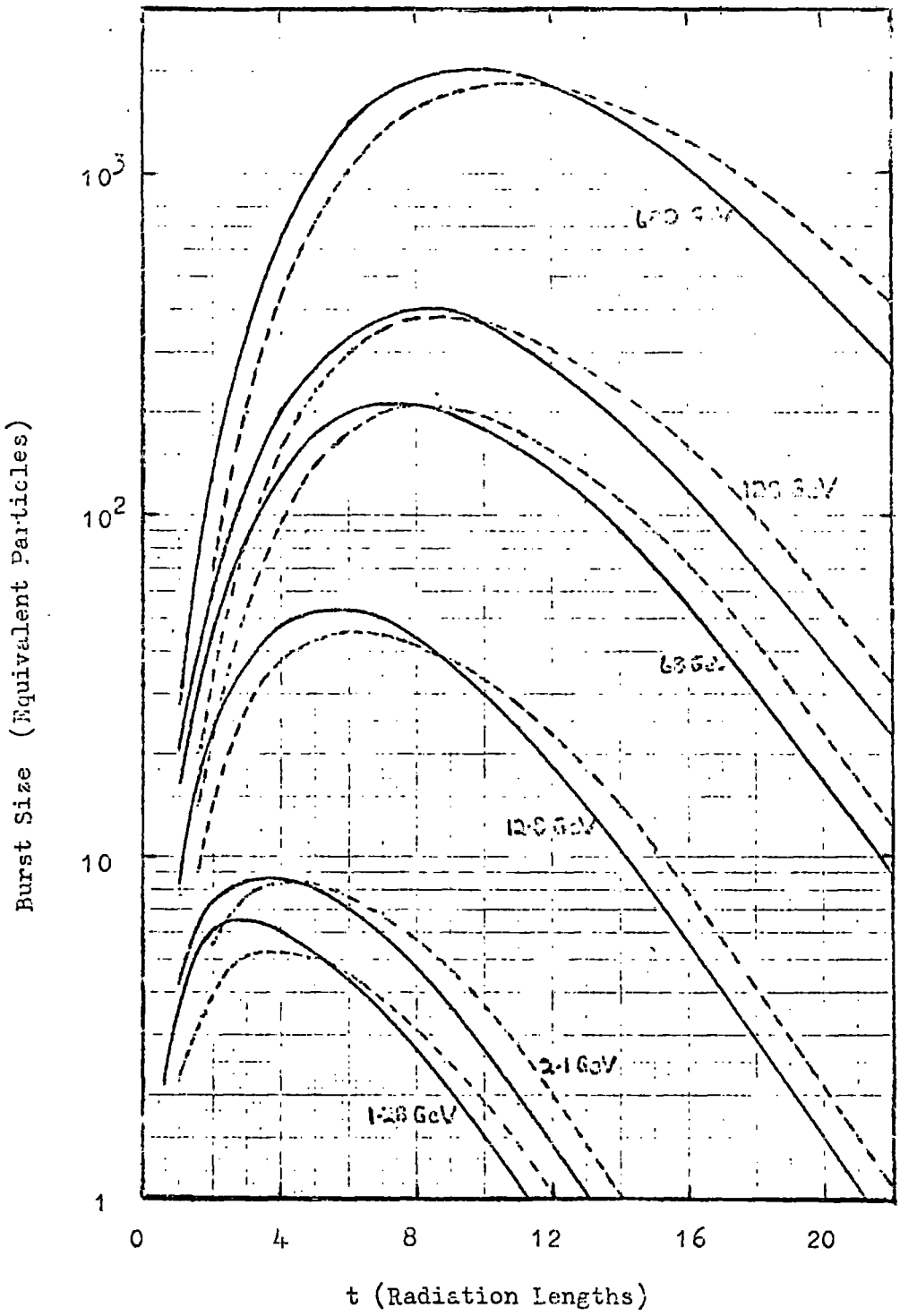

Figure 5.6 Shower development curves giving the burst size in equivalent particles recorded by the scintillator as a function of depth for cascades initiated by electrons (full lines) and photons (broken lines) of energies 1.28 , 2.1, 12.8 , 68, 128, and 680 GeV.

energy E_o GeV. The other $E_o/2$ is assumed to go into the production of pions. The number of pions produced has been calculated from $n_s = 3E_o^{\frac{1}{4}}$ with E_o in GeV and equal numbers of positive, negative and neutral pions are assumed to be produced. Equipartition of energy among the produced pions is also assumed. The neutral pions decay into two gamma rays, the charged pions either interacting deeper in the iron or emerging from it without interaction. Those that do interact produce more pions the multiplicity being given by $n_s = 3E_\pi^{\frac{1}{4}}$ with E_π in GeV. Equipartition of energy is again assumed and the inelasticity for π^* interactions has been taken as unity.

The elementary inelastic cross-sections for p-p and π-p interactions have been given by Morrison (1963) as 30 mb and 22 mb respectively. The resulting cross-sections for pion and proton interactions with an iron nucleus are 631 mb and 715 mb respectively, so the respective mean free paths for pions and protons in iron are 146 gm cm^{-2} and 129 gm cm^{-2} taking the density of iron as 7.6 gm/cc.

Two methods have been used in the calculation of burst sizes produced by nucleons of various energies. In the first relatively simple method the nucleons were considered to interact at one level calculated as an average depth in the iron and the charged pions then interacted at a greater depth also calculated as an average. In the second more detailed method different points of interaction were considered in the case of nucleons but the pions were still allowed to interact at an average depth. In both cases it was assumed that one

third of the pions produced in the interactions were π^0's and that these decayed into photons to initiate the cascade.

The processes in which the secondary particles from the interactions are generated are of a statistical nature so it would be expected that there will be large fluctuations in the measured energy loss. This is particularly true in an experiment such as the present where only a fraction of the energy is deposited in the detector. However, while the energy determination of an individual event may be unreliable it is still possible to measure a nucleon spectrum if the distribution function of these fluctuations is known.

5.4.2 Simple Treatment

Consider a high energy nucleon incident on an iron target of thickness X gm.cm^{-2}. Let λ_N represent the interaction length of nucleons in the iron. The probability that a nucleon interacts in the iron target is given by $\left[1 - \exp\left(\frac{-X}{\lambda_N}\right)\right]$. In this simpler treatment it has been assumed that all the nucleons which interact do so at one average depth. Calculation shows that on the average the distance after which the nucleons interact is given by

$$\bar{x}_N = \lambda_N - \frac{X}{\left[\exp\left(\frac{X}{\lambda_N}\right) - 1\right]}$$

Photon initiated cascades have been assumed to originate from this point and the curves of Figure 5.6 have been used to evaluate

the contribution to the burst size detected by the scintillator.

The charged pions produced in the nucleon-iron nucleus collision either interacted deeper in the iron or emerge from it without interaction. The number that do interact is given by

$$I_{\pi} = I_{o\pi} \left[1 - e^{-\left(\frac{X-\bar{x}_N}{\lambda_{\pi}}\right)} \right]$$

where $I_{o\pi}$ is the number of charged pions produced in the nucleon interaction and λ_{π} the mean free path for pion interactions in iron. It has again been assumed that the I_{π} pions interact at an average depth given by

$$\bar{x}_{\pi} = \lambda_{\pi} - \frac{(X-\bar{x}_N)}{\left[\exp\left(\frac{X-\bar{x}_N}{\lambda_{\pi}}\right)-1\right]}$$

One third of the pions produced in these secondary interations are again assumed to be π^0's and the curves of Figure 5.6 are used to evaluate the contribution to the burst size. No further nucleon collisions have been considered.

The relation between the energy of the interacting nucleon and the burst size detected by the scintillator has been evaluated in this way for several values of nucleon zenith angle. These curves are shown in Figure 5.7.

5.4.3 A More Detailed Treatment

In this method various points of interaction of the incident nucleons were considered. The charged pions which interacted deeper

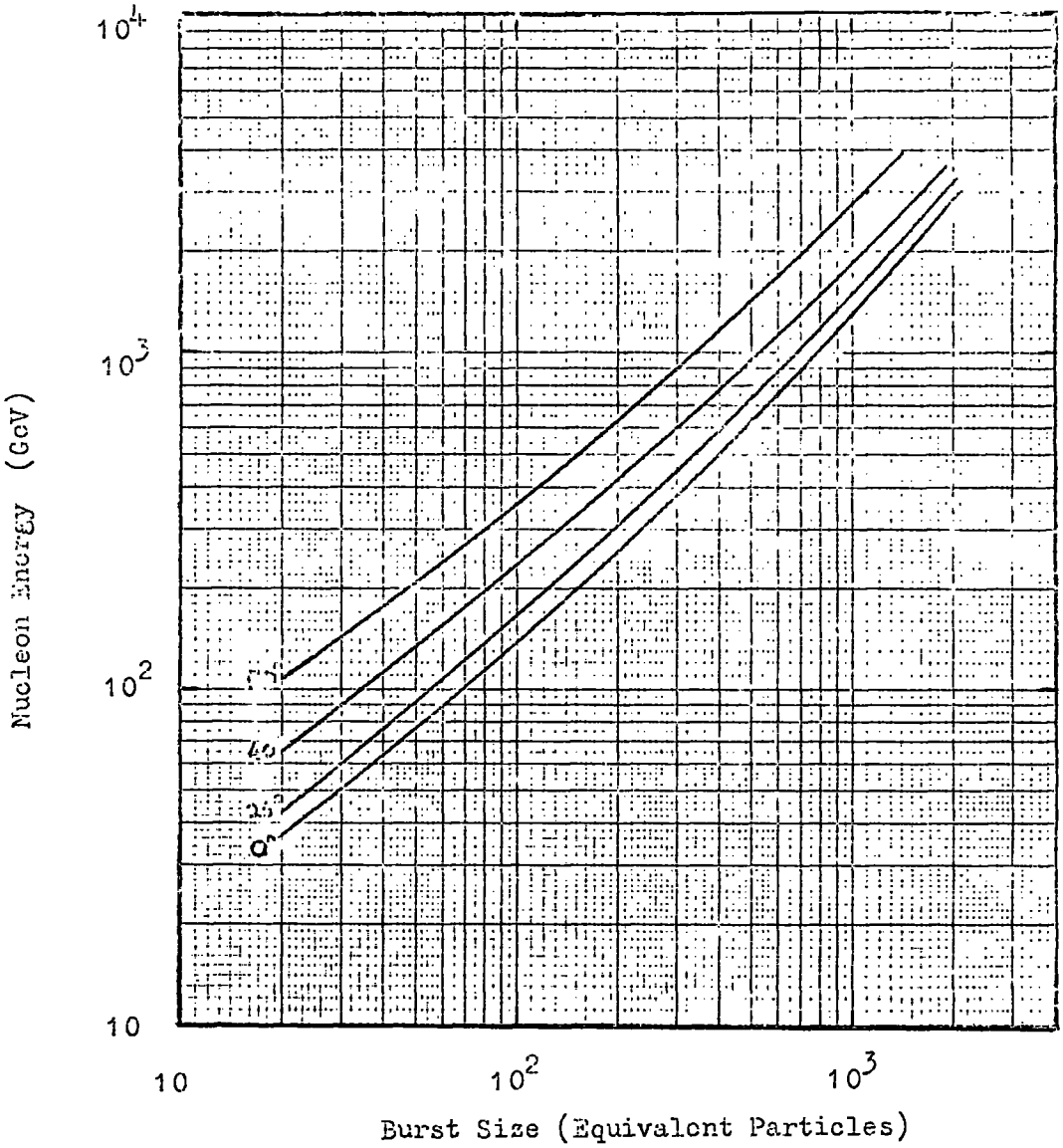

Figure 5.7 Burst Size - Energy Relationship for nucleons incident at various zenith angles on a 22.9 cm. thick iron target according to the more simple treatment.

in the iron were again considered to do so at some average depth which depended on the point of interaction of the nucleon. The variation of burst size recorded by the scintillation counter as a function of the point of interaction of the nucleon was thus obtained. These curves were then used to evaluate the probability per unit burst size of a nucleon of a given energy producing a given burst size. The mean values of these probability distributions were calculated. This procedure was carried out for a series of nucleon energies and zenith angles. These mean values were used in the plotting of the burst size energy relationship shown in Figure 5.8. A comparison is made with the results of the simpler treatment and it can be seen that in the more detailed calculation a given burst size corresponds to a nucleon of higher energy than in the case of the simpler method. Thus using this second method to convert burst size to energy will move the spectrum of nucleons to slightly higher energies.

5.4.4 Probability Distributions

In this experiment the burst size detected by the scintillator and which has been produced by a nucleon of a given energy depends on the point of interaction of the nucleon. The probability that a nucleon of a given energy produces a burst in a given burst size range can be evaluated. An example is shown in Figure 5.9 for the burst size range 130 to 260 equivalent particles. This has been

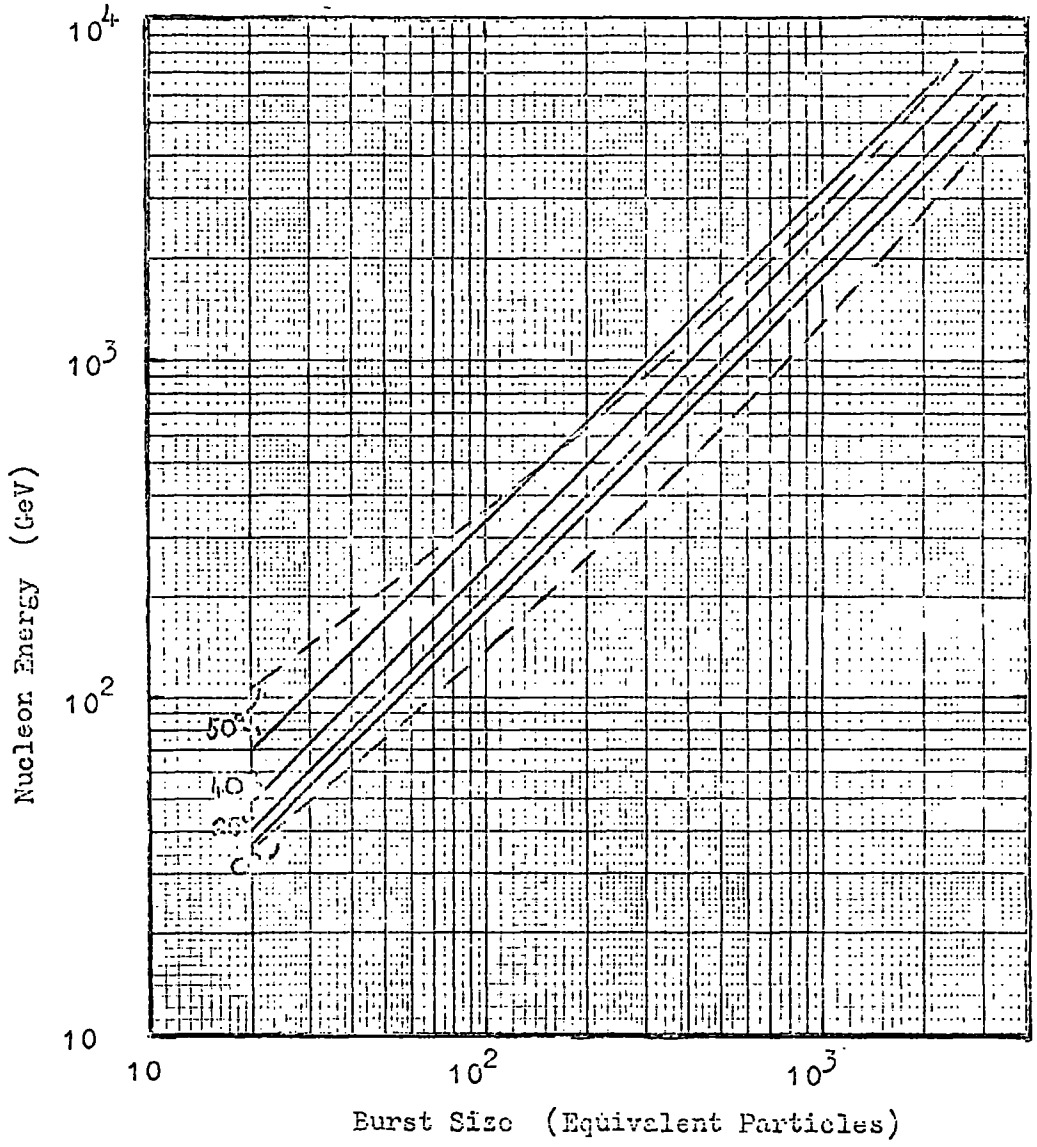

Figure 5.8 Burst Size - Energy Relationship for nucleons incident at various zenith angles on a 22.9 cm. thick iron target according to the more detailed calculation. (Full Lines).
— — — are the curves from the simpler treatment (Figure 5.7).

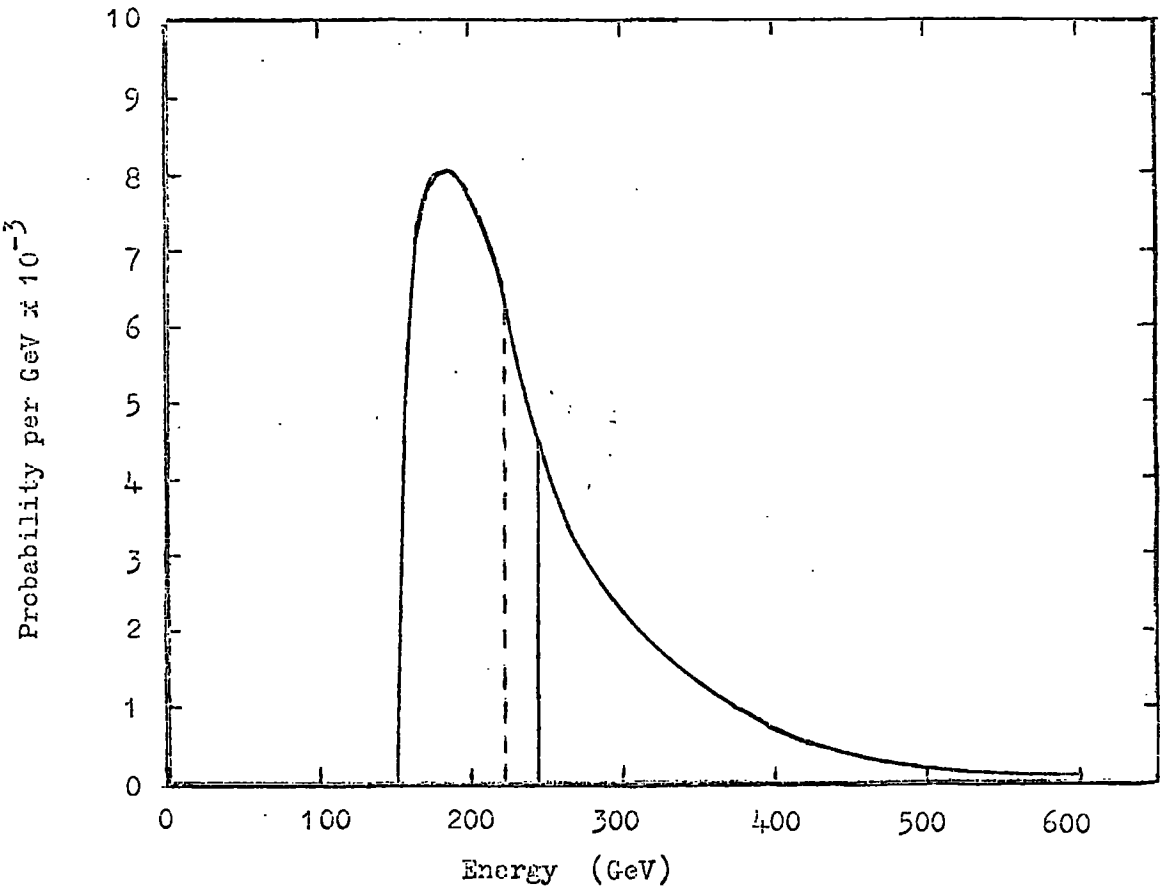

Figure 5.9 Probability of a nucleon of a given energy producing a burst size in the range 130 to 260 equivalent particles.

- - - Median

—— Mean

calculated using the cascade theory described earlier taking into account the varying probability of nucleons interacting at different points in the iron absorber and the fact that the nucleon spectrum is a rapidly falling one. For the purposes of this calculation the spectrum was assumed to have a differential exponent of -3.0 (that measured in the experiment).

5.5 Calculations of Pinkau and Thompson (1966)

In these calculations a series of curves have been produced which give the total number of electrons as a function of depth in various absorbers, one of which is iron. They used the nuclear interaction model described by Cocconi, Koester and Perkins (1961) (C.K.P. Model). Total electron numbers were calculated for different values of the nucleon inelasticity and multiplicity and it was found that the electron number at the shower maximum depended very little on the multiplicity. The curves have been adapted to apply to the present apparatus using a value of the nucleon inelasticity of 0.45 and 10 for the multiplicity. Account has been taken of the large reduction in electron number due to the transition effect when the electron cascade leaves the iron and enters the scintillator (Pinkau (1965)), and a 24% contribution from photon interactions in the phosphor has also been added. The relationship between burst size and nucleon energy calculated in this way is shown in Figure 5.10. The curves calculated from the shower theory of Ivanenko et al are

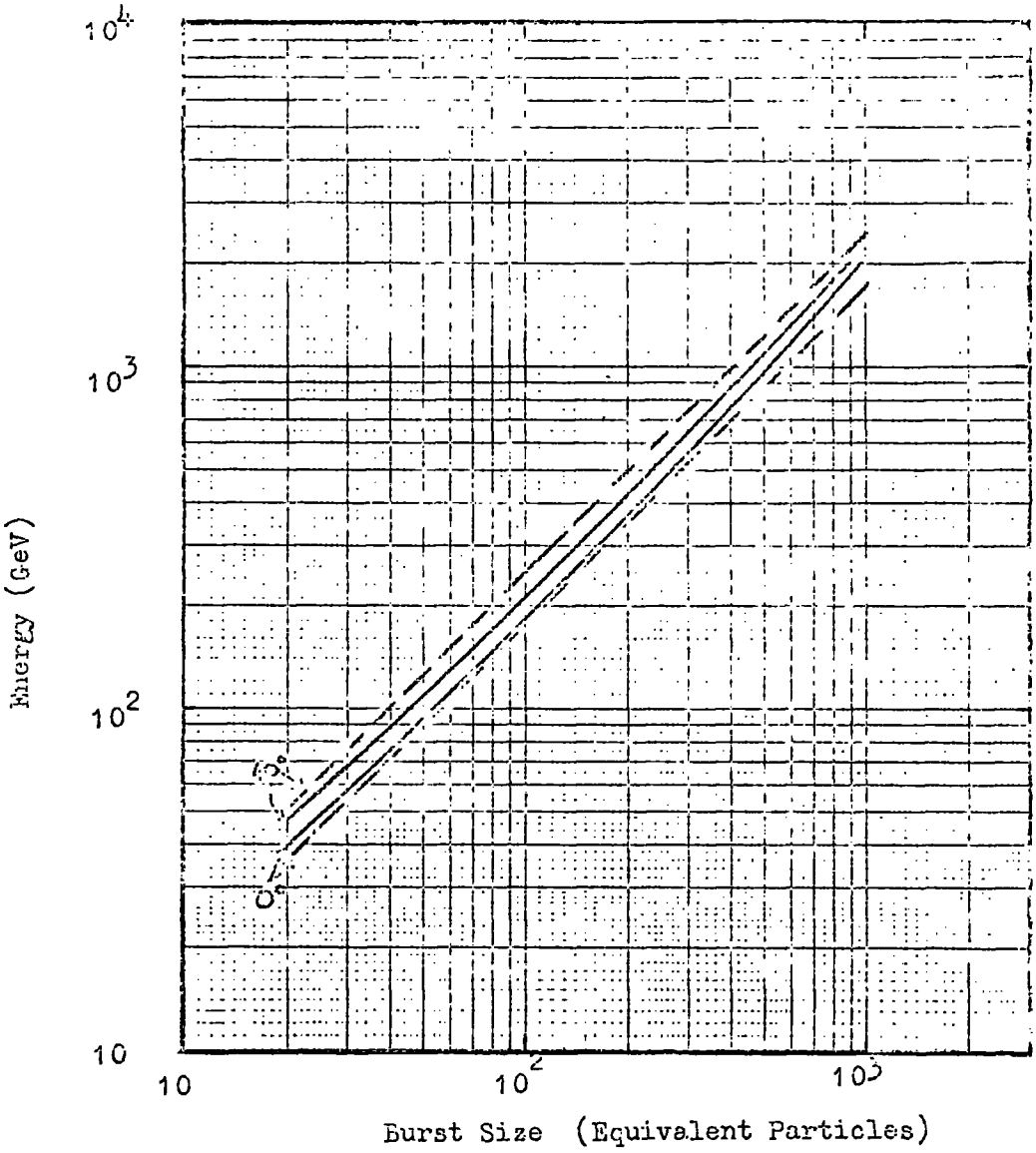

Figure 5.10 Burst Size - Energy Relationship adapted from the curves of Pinkau and Thompson (1966) (Full Line). The dashed lines represent the relationship calculated from the cascade curves of Ivanenko (Figure 5.8).

shown for comparison and it can be seen that there is quite good agreement between the two even though the conversion of Pinkau's data to apply to the present experiment was performed very simply. It will be seen later that there is little or no difference between the nucleon spectra calculated using these two sets of curves.

5.6 Experimental Studies Jones et al (1969) .

This group have assembled an ionisation spectrometer to study high energy cosmic rays at large altitudes. An experiment has been performed at the Brookhaven A.G.S. to calibrate the instrument with protons of momenta 10, 20.5, and 28 GeV/c. Normally ionisation calorimeters contain about ten interaction lengths of absorber which converts about 90% of the energy of the interacting particle into ionisation. The apparatus used by Jones et al contained only three interaction lengths mainly because it was flown in a balloon which set a limit on the weight that could be carried. This makes their results interesting to study with reference to the present apparatus as it contained only 1.35 interaction lengths. These show that over the momentum range covered there is an approximately linear relationship between the measured particle number and the energy of the interacting nucleon. The distribution of particle numbers for a given primary energy, however, is quite broad indicating that the errors involved are large. At the depth relevant to the neutron spectrum experiment the value of $\sigma/\bar{N}_i$, where σ is the standard deviation and $\bar{N}_i$ the

mean particle number, is about 50%.

5.7 Conclusions

The burst size to energy conversions evaluated using the cascade curves of Ivanenko et al have been used in the estimation of the sea level neutron spectrum. The results of Pinkau et al have also been used for the same purpose and a comparison of the two spectra will be made.

CHAPTER 6

THE EXPERIMENTAL ARRANGEMENT AND BASIC DATA

6.1 Introduction

The object of the present experiment has been to study burst production by neutral and charged nuclear active particles in the near vertical (zenith angles $< 60^{\circ}$) flux of the sea level cosmic radiation. A scale diagram of the apparatus is shown in Figure 6.1. It is a larger modified version of a preliminary experiment carried out by Ashton and Coats (1968) and consists of the following from top to bottom: eight layers of neon flash tubes (external diameter 1.8 cms), 22.9 cms of iron absorber, two layers of flash tubes in the front and two in the side elevation, three large adjacent 17 cm deep liquid paraffin scintillation counters and finally two more layers of crossed flash tubes. The major difference from the apparatus used by Ashton and Coats is the introduction of the flash tube trays in the side elevation which enables neutral induced bursts to be identified unambiguously; the area covered has also been increased three fold to 3.9 m^2. The iron absorber contains 1.35 interaction lengths (using λ_i = 129 gm cm^{-2}) so the probability of an incident vertical nucleon undergoing an interaction is 0.74. The burst produced as the result of the interaction of such a nucleon in the iron is detected by the scintillation counter. The pulse from the scintillator is used to select events above a predetermined level and also to calculate the

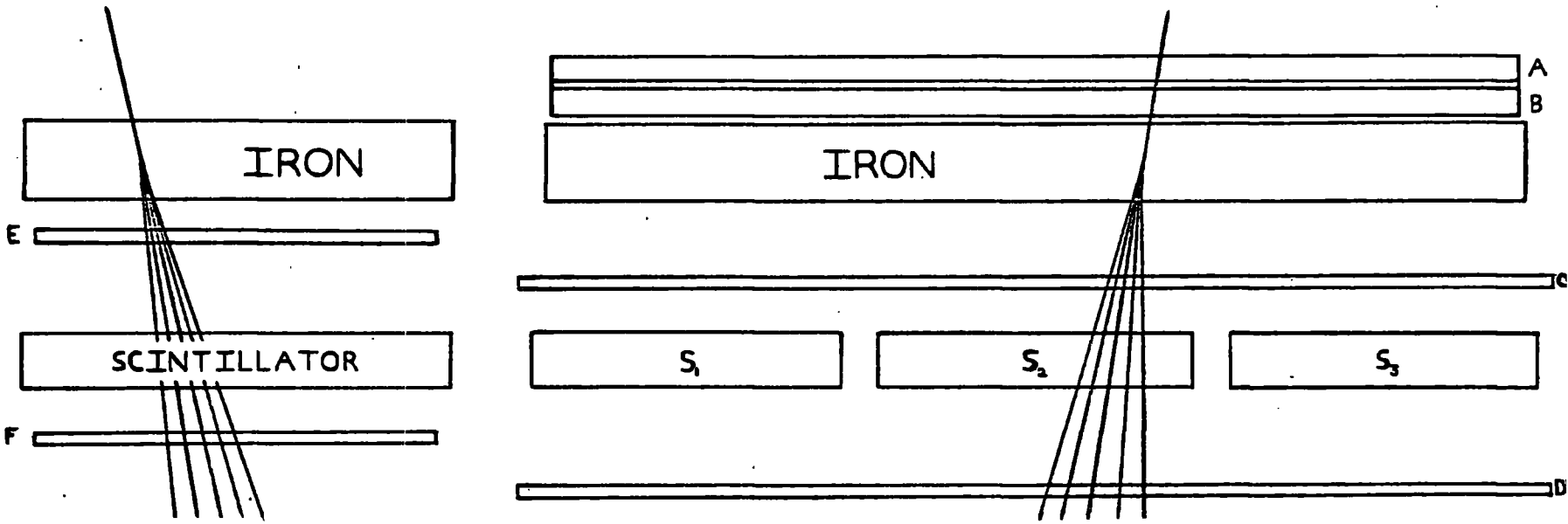

Figure 6.1 Scale Diagram of the Apparatus.

A, B, C, D, E, F, - Flash Tube Trays.
S_1, S_2, S_3 - Scintillation Counters.

size of the burst while the flash tubes give visual information about the event. In the interaction of the nucleons, pions are predominantly produced. The neutral pions decay into two gamma rays which then produce an electron-photon shower while the charged pions interact deeper in the iron to produce more charged and neutral pions. The burst detected by the scintillation counter thus consists of photons, electrons and pions.

6.2 The Scintillation Counters

Three of these were employed and each consisted of a liquid phosphor, medicinal paraffin plus 0.5 gm. per litre of p-terphenyl and 0.005 gm. per litre of POPOP, contained in a rectangular perspex box of dimensions 130 x 90 x 17.8 cm and a wall thickness of $\frac{3}{8}$ in. This box was placed in a larger light-tight wooden box being mounted on wooden rods so that the light transmitted through the phosphor to the photomultipliers was from total internal reflection. One of these counters is drawn to scale in Figure 6.2. Plane mirrors were placed along the sides AB, BC, DE, and EF of the wooden box and in a like manner at its other end. The phosphor was viewed by two 5 in. photomultipliers (E.M.I type 9583 B), one at each end of the box and and the air space enclosed by the plane mirrors acted as a light guide. A positive supply voltage was applied to the photomultipliers and the output pulse taken from the anode - this pulse being a negative one with a decay time of 1 μsec.

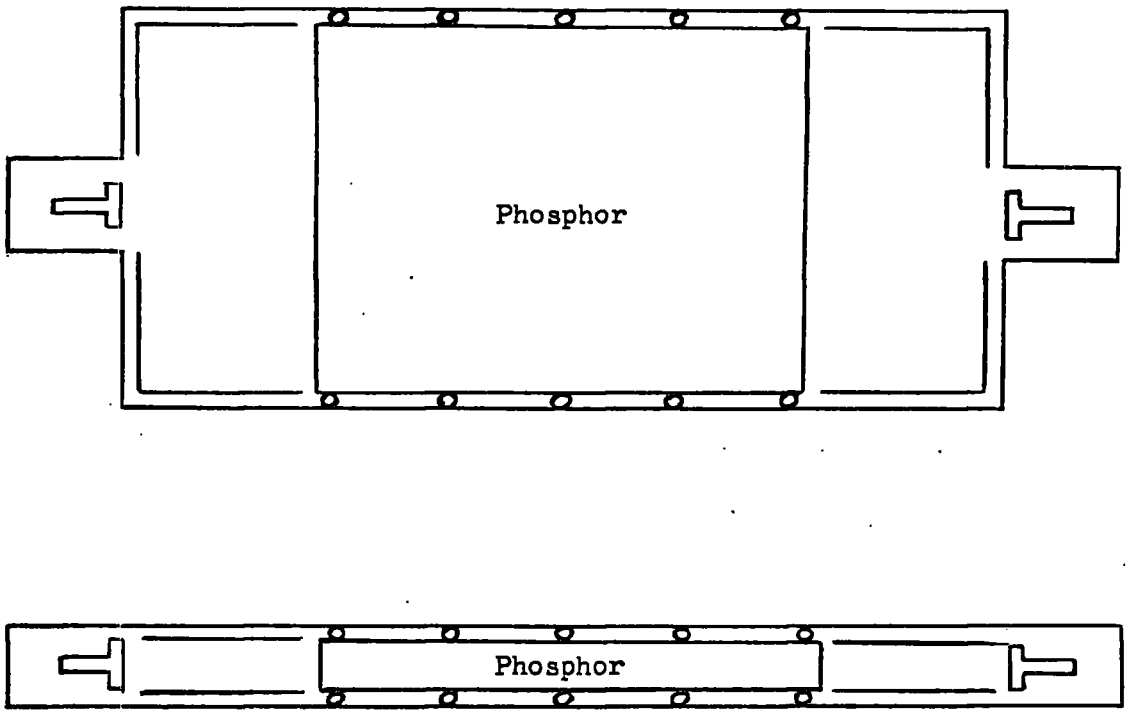

Figure 6.2 Scale Diagram of a Scintillation Counter.

In this type of experiment it is important that the response, i.e. the variation of pulse height with distance of the ionising particle from the photomultiplier, of the scintillator be fairly uniform. Scintillators of the type used in this experiment and in particular their response characteristics have been investigated by Ashton et al (1965). These results give a measure of the attenuation of the light in the phosphor. The experimental response curves show that with both photomultipliers in operation an ionising particle passing vertically through the centre of phosphor will on the average produce a pulse height which is 18% greater than that produced by a similar particle passing close to one end of the phosphor.

When the scintillators are operating under experimental conditions it is required that the two photomultipliers be matched, i.e. that their gains should be the same. Any mismatching leads to a broadening of the single particle distributions from the scintillation counter. Initially the matching of the gains of the photomultipliers was carried out as follows. Each photomultiplier was placed in turn in a light-tight box. Inside this box light pulses were produced by the arc-discharge of a mercury-wetted relay (Kerns et al (1959)). The variation of pulse height with supply voltage was measured for each tube and these results are shown in Figure 6.3. The photomultipliers were paired off as follows: I and E in scintillator S_1, A and C in S_2 and H and G in S_3. Figure 6.3 shows that while each photomultiplier had a different absolute gain the variation of this gain was of the

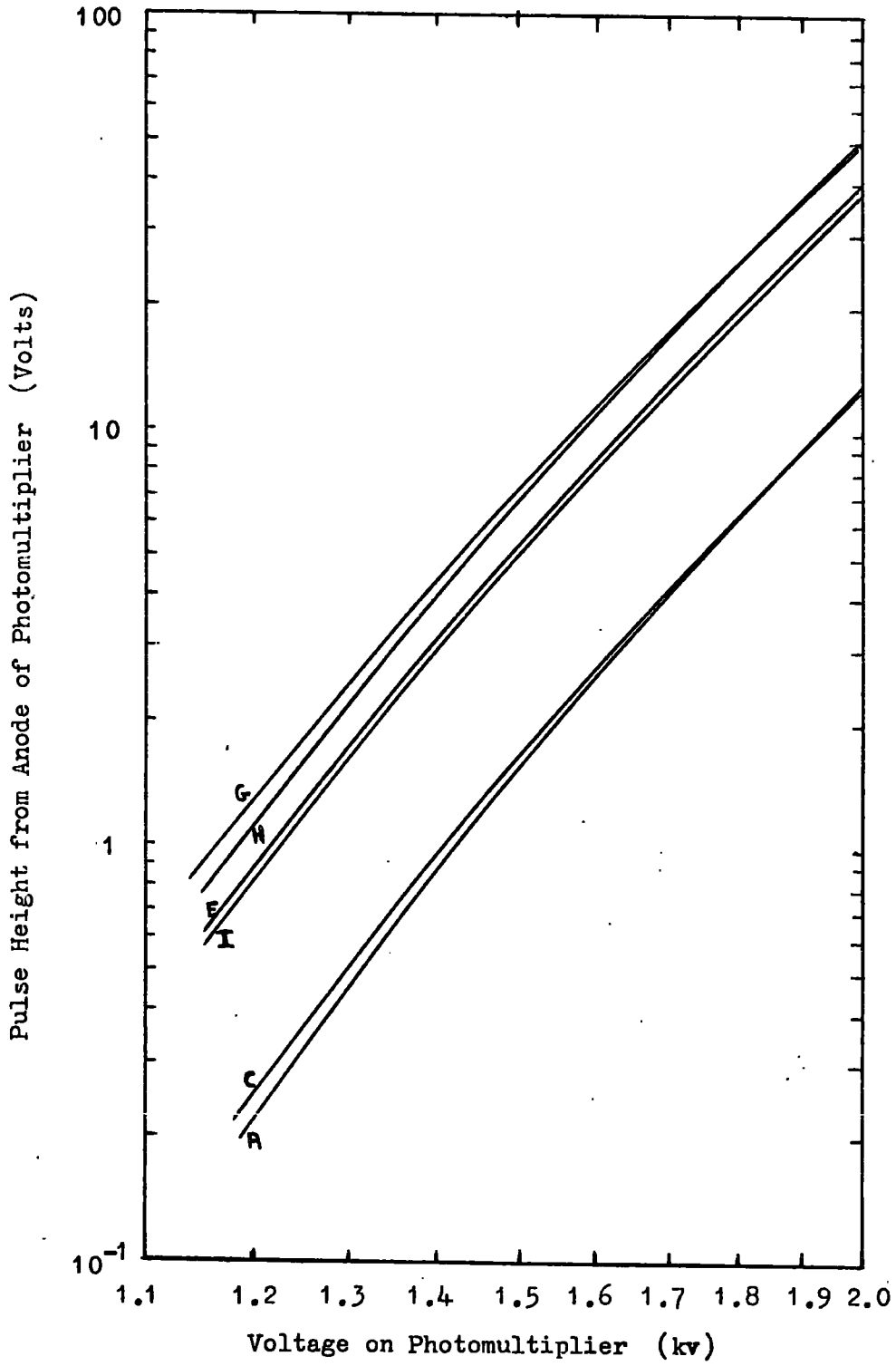

Figure 6.3 Response Characteristics of the Photomultipliers.

With the values of 6KV for the constant H.V. and 2KV for the pulse the efficiency of the counter was almost 100% for a time delay of the pulse of under 2μsec. For delays greater than 2μsec the efficiency fell off rapidly because the negative ions produced by the ionising particle were collected at the central wire before the application of the high voltage pulse.

B.3 Concluding Remarks

Several of the long proportional counters have been constructed and incorporated into the burst experiment described in this thesis. They are at present being used to determine the electric charge of incident charged particles that produce bursts.